1. Report No.	2. Government Accession No.	3. Recipient's Catalog No.
NASA CR-145209		

4. Title and Subtitle	5. Report Date
A Finite Element Algorithm for Sound Propagation in Axisymmetric Ducts Containing Compressible Mean Flow	June 1977
	6. Performing Organization Code

7. Author(s)	8. Performing Organization Report No.
A. L. Abrahamson	50624
	10. Work Unit No.

9. Performing Organization Name and Address	11. Contract or Grant No.
Wyle Laboratories 3200 Magruder Boulevard Hampton, Virginia 23666	NAS1-12841
	13. Type of Report and Period Covered
12. Sponsoring Agency Name and Address	Contractor Report
National Aeronautics and Space Administration Washington, D.C. 20546	14. Sponsoring Agency Code

15. Supplementary Notes

Final Report

16. Abstract

This report describes the development of an accurate mathematical model for sound propagation in axisymmetric aircraft engine ducts with compressible mean flow. The model is based on the usual perturbation of the basic fluid-mechanics equations for small motions. Mean flow parameters are derived in the absence of fluctuating quantities and are then substituted into the equations for the acoustic quantities which were linearized by eliminating higher order terms. Mean swirl is assumed to be zero from the restriction of axisymmetry.

A linear rectangular "serendipity" element is formulated from these equations using a Galerkin procedure and assembled in a special purpose computer program in which the matrix map for a rectangular mesh was specifically coded. Representations of the fluctuating quantities, mean quantities and coordinate transformations are isoparametric. The global matrix is a block tridiagonal system of which the blocks are themselves banded matrices. The global matrix is held in packed form both in core and on secondary storage and is solved by foreward and back substitution following an L-U decomposition with pivoting restricted internally to the blocks. Results from the model were compared with results from several alternative analyses and yielded satisfactory agreement. The method is sufficiently fast to permit novel optimization studies on a variety of duct parameters.

17. Key Words (Suggested by Author(s))	18. Distribution Statement
Acoustic Finite Element Duct Acoustics Large Linear Systems	Unclassified - Unlimited

19. Security Classif. (of this report)	20. Security Classif. (of this page)	21. No. of Pages	22. Price*
Unclassified	Unclassified	687	

*For sale by the National Technical Information Service, Springfield, Virginia 22151

TABLE OF CONTENTS

		Page
	Notations and Definitions	v
1.0	INTRODUCTION	1
2.0	DESCRIPTION OF MATHEMATICAL MODEL	4
2.1	Problem Formulation	4
2.2	Solution Strategy	9
2.3	Element Derivation	16
2.4	Algebraic Integration for Ducts of Constant Cross-Sectional Area	22
2.5	Numerical Integration for Arbitrary Axisymmetric Ducts	25
2.6	Global Matrix Assembly, Packing Technique, and Insertion of Boundary Conditions	27
2.7	Solution of Matrix Equation	30
3.0	DESCRIPTION OF RESULTS	37
3.1	Comparison of Model with Previous Analyses	37
3.2	Illustrations of Potential of Current Model in Duct Optimization	42
3.2.1	Quadratic Liner Variation	42
3.2.2	Optimization of a Convergent-Divergent Duct	42
3.2.3	Optimization with a Center Body	44
3.3	Computing Time	48
4.0	CONCLUSIONS	50
REFERENCES		52
	APPENDIX	
1	Area Element Coordinate Transformation	55
2	Definition of Terms Used in Equations (46) through (49)	56
3	Abscissae and Weight Coefficients of the Gaussian Quadrature Formula	59
4	Listing of Subroutine PINDS	60
5	Termination Boundary Condition	61
6	Insertion of a Noise Source Boundary Condition	64
7	Insertion of an Admittance Boundary Condition. (Figure 7-1 Orientation of Acoustic Velocities and Boundary Wall)	64
8	Linear Numerical Flux Integration	68

LIST OF FIGURES AND TABLES

Figure		Page
1	Typical Engine Duct	2
2	Serendipity Element	11
3	Rectangular Discretization in Plane	13
4	Matrix Map of the 2-D Rectangular Discretization of Figure 3	14
5	Deformed Element	18
6	Logic Diagram for Evaluation of Integrals	28
7	Description of Block Tridiagonal Matrix Solution with Memory Map	34
8	Comparison of Acoustic Attenuation vs. Mesh Density with Exact Solution Computed from Work of Zorumski [15]	38
9	Comparison of Pressure Variation with Axial Distance Derived from Morse's Analysis for a Conical Horn with Results from the Current Model	41
10	Admittance Variation with Axial Coordinate for Quadratic Liner	43
11	Plot Showing Envelopes of Pressure Amplitudes with Axial Distance at Selected Radial Stations	46
12	Constant Cross-Section Area Inlet Duct with Center Body	47
13	Plot of Central Processor Time (CDC Cyber 175) vs. Matrix Order	49

Table		
I	Comparison of Optimum Acoustic Liner Determinations	39
II	Comparison of Duct Attenuations in Presence of Plug Flow	39

ACKNOWLEDGEMENTS

The author would like to express his particular thanks to Mr. Laurence Keefe for many useful conversations, assisting in development of some of the equations, and in the preparation of the report. He would also like to express his appreciation to Drs. William E. Zorumski, Harold C. Lester and members of the Acoustics Branch, Acoustics and Noise Reduction Division, NASA Langley Research Center for useful comments and advice throughout the course of the work.

Notations and Definitions

$(\;)$	Row vector.
$\{ \; \}$	Column vector.
$[\;]$	Matrix.
$(\;)^*$	An asterisk as a variable superscript indicates complex conjugate.
$\overline{(\;)}$	A bar over a variable indicates a mean flow quantity.
$\tilde{(\;)}$	A tilda over a variable indicates a nondimensional quantity.
$(\;)'$	A prime as a variable superscript indicates time dependence.
$\vec{(\;)}$	An arrow over a variable indicates a vector.
$\langle \; \rangle$	Indicates time average quantity.

List of Symbols

$A, B, C \ldots Q$	Scalar quantities defined by equation (50).
(H_i, H_i')	Gaussian quadrature weights.
c	Speed of sound.
F_s	Acoustic flux through source plane.
F_r	Acoustic flux through radiation plane.
f	Frequency.
I	Acoustic intensity.
I_z	Z-component of acoustic intensity
$[I]$	Identity matrix.
i	Index.
$[J]$	Jacobian matrix.

$\|J\|$	Determinant of Jacobian.
j	Index.
ℓ	Number of variables per node.
M	Mach number on axial direction.
M'	Radial derivative of M $\left(= \frac{\partial M}{\partial r}\right)$
m	Number of nodes in serial numbering direction.
N	Linear function for serendipity element.
P	Pressure (unperturbed equations)
P_r	Prandtl number.
p	Pressure (acoustic variable)
Q	Transformed constriction parameter.
q	Constriction parameter.
R_o	Outer duct radius at $z = o$
R_e	Reynolds number.
r	Radial coordinates.
T	Temperature.
t	Time.
$\vec{V}$	Velocity vector.
(U, V, W) (z, r, θ)	Velocity components (mean flow and unperturbed equations).
$(u \quad v \quad w)$ (z, r, θ)	Acoustic velocity components
z	Axial coordinate.

List of Symbols (cont'd)

α_z, α_r	Defined by equation (26).
β	Admittance.
$[\alpha], [\beta], [\gamma], [\delta], [\mu]$	Defined in Appendix 2.
γ	Gas specific heat ratio.
ε	Impedance of air $(= \bar{\rho} c)$
η	Local coordinate
η_i	Gauss abscissa point.
θ	Circumferential coordinate.
κ	Gas thermal conductivity.
λ	Wavelength.
ξ	Local coordinate (axial direction)
ξ_i	Gauss abscissa point.
ρ	Density (unperturbed equations).
$\bar{\rho}$	Density.
$\underline{\underline{\tau}}$	Dimensionless viscous stress tensor.
ϕ	Dimensionless dissipation function.
ω	Angular frequency.

1.0 INTRODUCTION

The objective of the work described in this report was the development of a finite element scheme applicable to the acoustics of aero-engine ducts. The finite element method, which is widely used with considerable success in structural mechanics, is currently finding applications in all areas of continuum mechanics.

The application of finite element methods to acoustics is not new. A significant amount of work has already been performed in determining the acoustic modes of closed cavities and in determining the response of coupled acoustic-structural systems (references 1-9). These analyses assumed simple acoustic systems in a uniform medium with no mean flow. Under these circumstances it was possible to formulate variational principles which were then used as the basis for a finite element model. None of these assumptions are valid within a modern aircraft engine such as shown in Figure 1. Here, the noise generation mechanisms are complex, and the medium which transmits the sound contains large gradients and moves with a considerable velocity. Since no variational principal exists for acoustic fluctuations in such a medium, an acoustic analysis must proceed directly from the differential equations which describe compressible flow.

From a cursory examination of the physical size of fan engine ducts on current aircraft, and from the knowledge that predominant fan tones exceed 2000Hz, it is clear that the principal difficulty in development of an acoustic model on existing computers is the sheer scale of the required model. In structural mechanics after 20 years of experience, 10 000 degrees of freedom still represent a large problem. At the outset, it is apparent that the acoustic model will require upwards of 100 000 degrees of freedom.

This is not the only complication, because in structural mechanics as well

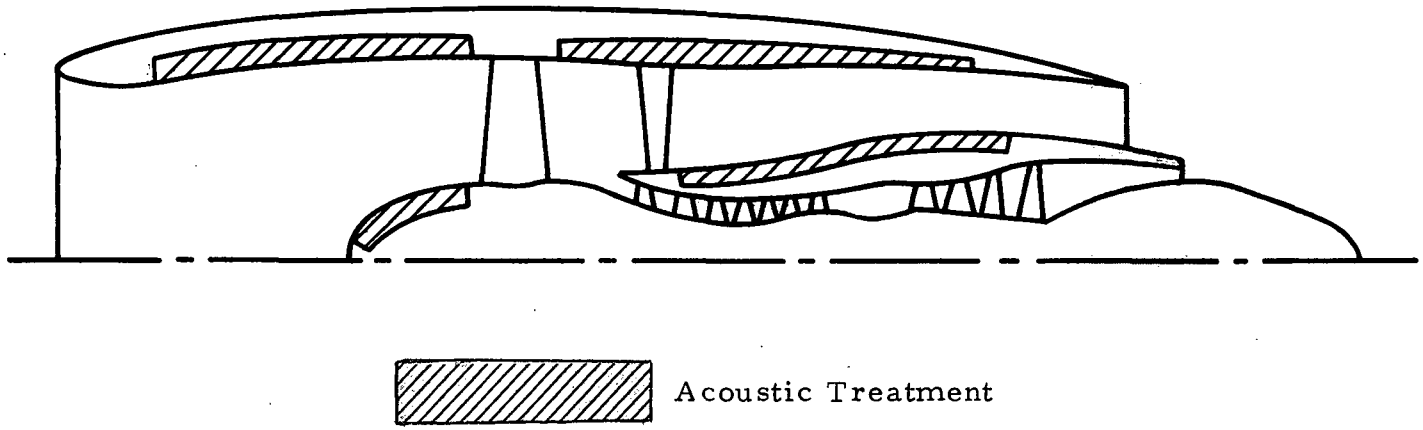

Figure 1. Typical Engine Duct.

as in previous acoustic studies, global finite element matrices possess desirable properties, being generally real, symmetric, and positive-definite. The symmetric, positive-definite form results from the variational formulation on which the finite element models are based. However, the Galerkin variation of the method of weighted residuals used for the acoustic element in this work produces matrices which are complex, non-Hermitian and nonpositive-definite. Matrices of this type require special techniques to avoid numerical errors in their solution. These techniques are less plentiful than for symmetric positive-definite matrices and become difficult to implement efficiently for large matrix orders.

This report describes a solution to the problems outlined above, describes the development of a finite element model, and shows typical results derived from this model.

2.0 DESCRIPTION OF MATHEMATICAL MODEL

2.1 Problem Formulation

The purpose of this analysis is the calculation of sound propagation in axisymmetric ducts containing compressible flow. The nondimensional equations governing the motion of the fluid are:

Conservation of Momentum

$$\tilde{\rho}\left(\frac{\partial \vec{\tilde{V}}}{\partial t} + (\vec{\tilde{V}}\cdot\vec{\nabla})\vec{\tilde{V}}\right) = -\vec{\nabla}\tilde{p} + \frac{1}{Re}\vec{\nabla}\cdot\underline{\underline{\tau}} \tag{1}$$

Conservation of Mass

$$\frac{\partial \tilde{\rho}}{\partial t} + \vec{\nabla}\cdot(\tilde{\rho}\vec{\tilde{V}}) = 0 \tag{2}$$

Conservation of Energy

$$\tilde{\rho}\left(\frac{\partial \tilde{T}}{\partial t} + \vec{\tilde{V}}\cdot\vec{\nabla}\tilde{T}\right) - (\gamma-1)\left(\frac{\partial \tilde{p}}{\partial t} + \vec{\tilde{V}}\cdot\vec{\nabla}\tilde{p}\right) = \frac{1}{Re}\left\{\frac{1}{Pr}\vec{\nabla}\cdot(K\vec{\nabla}\tilde{T}) + (\gamma-1)\phi\right\} \tag{3}$$

Equation of State

$$\gamma\tilde{p} = \tilde{\rho}\tilde{T} \tag{4}$$

Equations (1) through (4) were made nondimensional for simplicity by using an arbitrary characteristic length; the ambient values of temperature, density, and speed of sound; and arbitrary characteristic values of viscosity and thermal conductivity. These equations govern both the mean flow and imposed acoustic motion within the duct.

While determination of the mean flow is necessary for solution of the acoustic problem, the assumptions and techniques used to obtain the mean solution are not part of this paper. Instead, it is assumed that the mean flow has already been obtained and is in suitable form for inclusion in the acoustic problem. At the same time, it is necessary to note that some terms in the equations (those involving viscosity and heat conduction) which may be important in deriving the mean flow solution are not of primary significance in determining the acoustic motion. Thus, while these terms might be retained for solution of the mean flow problem, they are eliminated here at the outset to simplify derivation of the equations describing the acoustic motion.

To begin this derivation, we write equation (1) in dimensional component form in cylindrical coordinates (ignoring viscosity).

Axial Direction

$$\rho\left(\frac{\partial U}{\partial t} + V\frac{\partial U}{\partial r} + \frac{W}{r}\frac{\partial U}{\partial \theta} + U\frac{\partial U}{\partial z}\right) = -\frac{\partial P}{\partial z} \tag{5}$$

Radial Direction

$$\rho\left(\frac{\partial V}{\partial t} + V\frac{\partial V}{\partial r} + \frac{W}{r}\frac{\partial V}{\partial \theta} - \frac{W^2}{r} + U\frac{\partial V}{\partial z}\right) = -\frac{\partial P}{\partial r} \tag{6}$$

Circumferential Direction

$$\rho\left(\frac{\partial W}{\partial t} + V\frac{\partial W}{\partial r} + \frac{W}{r}\frac{\partial W}{\partial \theta} + \frac{VW}{r} + U\frac{\partial W}{\partial z}\right) = -\frac{1}{r}\frac{\partial P}{\partial \theta} \tag{7}$$

Equation (2) becomes:

$$\frac{\partial P}{\partial t} + U\frac{\partial P}{\partial z} + V\frac{\partial P}{\partial r} + W\frac{\partial P}{\partial \theta} + \rho\left(\frac{\partial U}{\partial z} + \frac{\partial V}{\partial r} + \frac{1}{r}\frac{\partial W}{\partial \theta}\right) + \frac{PV}{r} = 0 \tag{8}$$

Assuming that all dependent variables are the sum of two motions; one the steady mean flow and the other a fluctuating acoustic motion, we write

$$\begin{aligned} P &= \overline{P}(r,\theta,z) + p'(r,\theta,z,t) \\ \rho &= \overline{\rho}(r,\theta,z) + \rho'(r,\theta,z,t) \\ U &= \overline{U}(r,\theta,z) + u'(r,\theta,z,t) \\ V &= \overline{V}(r,\theta,z) + v'(r,\theta,z,t) \\ W &= \overline{W}(r,\theta,z) + w'(r,\theta,z,t) \end{aligned} \tag{9}$$

Substituting equations (9) into equations (5) through (8), we derive two sets of equations: the first by assuming that the primed quantities are zero, and the second by using the full form of equation (9). Subtracting the first set from the second, ignoring second-order terms in the primed quantities and assuming mean swirl ($\overline{W}$) to be zero, we get

$$\begin{aligned} &\overline{\rho}\frac{\partial u'}{\partial t} + (\overline{\rho}v' + \rho'\overline{V})\frac{\partial \overline{U}}{\partial r} + \overline{\rho}\,\overline{V}\frac{\partial u'}{\partial r} \\ &\quad + (\overline{\rho}u' + \rho'\overline{U})\frac{\partial \overline{U}}{\partial z} + \overline{\rho}\,\overline{U}\frac{\partial u'}{\partial z} + \frac{\partial p'}{\partial z} = 0 \end{aligned} \tag{10}$$

$$\bar{\rho}\frac{\partial v'}{\partial t} + (\bar{\rho}v' + \rho'\bar{V})\frac{\partial \bar{V}}{\partial r} + \bar{\rho}\bar{V}\frac{\partial v'}{\partial r}$$

$$+ (\bar{\rho}u' + \rho'\bar{U})\frac{\partial \bar{V}}{\partial z} + \bar{\rho}\bar{U}\frac{\partial v'}{\partial z} + \frac{\partial p'}{\partial r} = 0 \qquad (11)$$

$$\bar{\rho}\left\{\frac{\partial w'}{\partial t} + \bar{V}\left(\frac{\partial w'}{\partial r} + \frac{1}{r}w'\right) + \bar{U}\frac{\partial w'}{\partial z}\right\} + \frac{1}{r}\frac{\partial p'}{\partial \theta} = 0 \qquad (12)$$

$$\frac{\partial \rho'}{\partial t} + \bar{U}\frac{\partial \rho'}{\partial z} + \bar{V}\frac{\partial \rho'}{\partial r} + u'\frac{\partial \bar{\rho}}{\partial z} + v'\frac{\partial \bar{\rho}}{\partial r}$$

$$+ \bar{\rho}\left(\frac{\partial u'}{\partial z} + \frac{\partial v'}{\partial r} + \frac{1}{r}\frac{\partial w'}{\partial \theta} + \frac{v'}{r}\right)$$

$$+ \rho'\left(\frac{\partial \bar{U}}{\partial z} + \frac{\partial \bar{V}}{\partial r} + \frac{\bar{V}}{r}\right) = 0 \qquad (13)$$

The neglect of viscosity and heat conduction in the acoustic motion means that it is an adiabatic process. When such is true, the energy equation and equation of state may be manipulated to give (Ref. 10, 11)

$$p' = \rho' c^2 \qquad (14)$$

Here c is the local speed of sound which is determined from the mean flow by the relation

$$c = \left(\frac{\gamma \bar{P}}{\bar{\rho}}\right)^{1/2} \qquad (15)$$

Assuming that $c = c(r, z)$, we may use equation (14) to eliminate ρ' from equations (10) through (13). Taking a harmonic solution in t and θ for the fluctuating quanties

$$(u', v', w', p') = (u, v, w, p)\, e^{\omega t + m\theta} \tag{16}$$

where ω and m are pure imaginary, the four equations governing the linearized acoustic motion in a nonuniform axisymmetric duct become

$$\omega u + \left(v + \frac{p\bar{V}}{\bar{\rho}c^2}\right)\frac{\partial \bar{U}}{\partial r} + \bar{V}\frac{\partial u}{\partial r} + \left(u + \frac{p\bar{U}}{\bar{\rho}c^2}\right)\frac{\partial \bar{U}}{\partial z} + \bar{U}\frac{\partial u}{\partial z} + \frac{1}{\bar{\rho}}\frac{\partial p}{\partial z} = 0 \tag{17}$$

$$\omega v + \left(v + \frac{p\bar{V}}{\bar{\rho}c^2}\right)\frac{\partial \bar{V}}{\partial r} + \bar{V}\frac{\partial v}{\partial r} + \left(u + \frac{p\bar{U}}{\bar{\rho}c^2}\right)\frac{\partial \bar{V}}{\partial z} + \bar{U}\frac{\partial v}{\partial z} + \frac{1}{\bar{\rho}}\frac{\partial p}{\partial r} = 0 \tag{18}$$

$$\omega w + \bar{V}\left(\frac{\partial w}{\partial r} + \frac{1}{r}w\right) + \bar{U}\frac{\partial w}{\partial z} + \frac{m}{\bar{\rho}r}p = 0 \tag{19}$$

$$\frac{\omega}{c^2}p + \frac{\bar{U}}{c^2}\left(\frac{\partial p}{\partial z} - \frac{2p}{c}\frac{\partial c}{\partial z}\right) + \frac{\bar{V}}{c^2}\left(\frac{\partial p}{\partial r} - \frac{2p}{c}\frac{\partial c}{\partial r}\right) + u\frac{\partial \bar{\rho}}{\partial z}$$

$$+ v\frac{\partial \bar{\rho}}{\partial r} + \bar{\rho}\left(\frac{\partial u}{\partial z} + \frac{\partial v}{\partial r} + \frac{m}{r}w + \frac{v}{r}\right) + \frac{p}{c^2}\left(\frac{\partial \bar{V}}{\partial z} + \frac{\partial \bar{V}}{\partial r} + \frac{\bar{V}}{r}\right) = 0 \tag{20}$$

2.2 Solution Strategy

Solution of equations (17) through (20) is not possible algebraically except with severely restrictive assumptions. The question is thus not whether to use a numerical technique for their solution, but rather which numerical technique to use.

Within each branch of applied science, partly from its historical development and partly from rational grounds, there appears to exist a favorite numerical method. Perhaps it is fortuitous that the rebirth of acoustics is too recent to have allowed development of any such prejudice.

For example, a variety of numerical techniques are used in connection with the problem of sound propagation in ducts. Mungur, in his work with Plumblee [10] and Gladwell [11] used a fourth-order Runge-Kutta approach. More recently, Baumeister, with Bittner [12] and with Rice [13] used an integral formulation to generate finite difference approximations to the differential equations. A more indirect technique involving modal expansions was used by Zorumski [14, 15]. Also in this vein is the wave envelope technique of Nayfeh, Shaker, and Kaiser [16] which reduces in the limit to the method of multiple scales of the earlier work of Nayfeh and Telionis [17].

Direct numerical solutions are subject to the problem of size. As pointed out by Nayfeh, Shaker, and Kaiser [16] for a negative Mach number tending to unity in magnitude, and high frequency, the number of axial steps required to resolve the quasi-sinusoidal spatial variation of the fluctuating parameters becomes very large.

No study has yet been conducted, however, to accurately determine the limits of direct numerical solutions using currently available computers.

This work began with the objective of determining these limits, using carefully determined storage and matrix manipulation algorithms in conjunction with a straightforward discretization scheme.

Due to the promising results obtained by finite-element algorithms in other fields of continuum mechanics and from initially promising applications to acoustics, finite elements were the medium chosen for this study.

The great majority of development of the finite-element method has taken place within the context of structural mechanics. Concerning the relative advantage of various types of elements, it is informative to note the comments of a specialist in this field: Zienkiewicz (Ref. 18, page 104) who states that, "The question may well be asked as to whether any economic or other advantage is gained by increasing the complexity of an element. The answer here is not any easy one, although it can be stated as a general rule that as the order of an element increases so the total number of unknowns in a problem can be reduced for a given accuracy of representation. Economic advantage requires, however, a reduction of total computations and data preparation effort and this does not follow automatically for a reduced number of total variables as, though equation solving times may be reduced, the time required for element formulation increases. In general, the optimum element may have to be determined from case to case."

In the light of these comments and for the sake of simplicity, a linear rectangular element from Zienkiewicz's Serendipity family (Ref. 18, page 107) was chosen as the basis for the analysis. Figure 2, contains a description of the nodal numbering system for the element, and shows orientation of local (η, ξ) coordinates and global (r, z) coordinates. (Since we assumed a harmonic angular (θ) dependence by equation (16), only a two-dimensional discretization is required.)

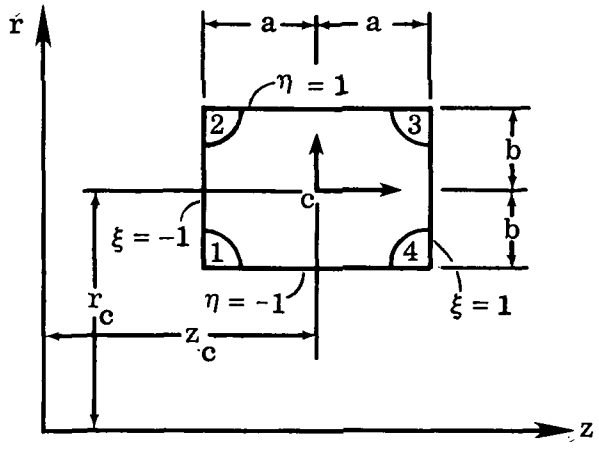

Figure 2. Serendipity Element.

A uniform discretization mesh for a duct of constant cross-sectional area is shown in Figure 3(a). The matrix map generated for this discretization by a nodal numbering system such as that shown in the figure may be developed as follows. Within each of the linear elements, interactions among nodal variables will only occur between those variables at the corners of the rectangle. Thus in element (2, 4), four sets of linear equations will link the four sets of nodal variables located at nodes 14, 15, 24, and 25. Consider the equation set representing variables at node 25. On assembly of the global matrix, this set will contain contributions from four adjacent elements namely (2, 4), (2, 5), (3, 4), (3, 5). That is, in the global matrix the variables at node 25 will be linked explicitly with variables at nodes 14, 15, 16, 24, 25, 26, 34, 35, 36. All other coefficients in the submatrix representing the equation set for variables at node 25 will be zero. For the case of "ℓ" parameters per node, the matrix map generated by linear elements and the rectangular discretization numbered as shown in Figure 3(a), is given in Figure 4.

The principal generalized characteristics evident from the map shown in Figure 4 may be summarized as follows:

- Global matrix consists of three diagonal bands.
- Width of each band is "3ℓ".
- Global matrix is block tridiagonal.
- Major blocks are themselves block tridiagonal.
- Order of major blocks is "$n\ell$" where "n" is equal to the number of nodes per row in the serial numbering direction.
- Order of minor blocks is "ℓ".

Although the characteristics of a matrix conforming to a generalized map such as that described above are extremely convenient for minimizing storage requirements, and computational effort during assembly and

(a) Uniform Rectangular

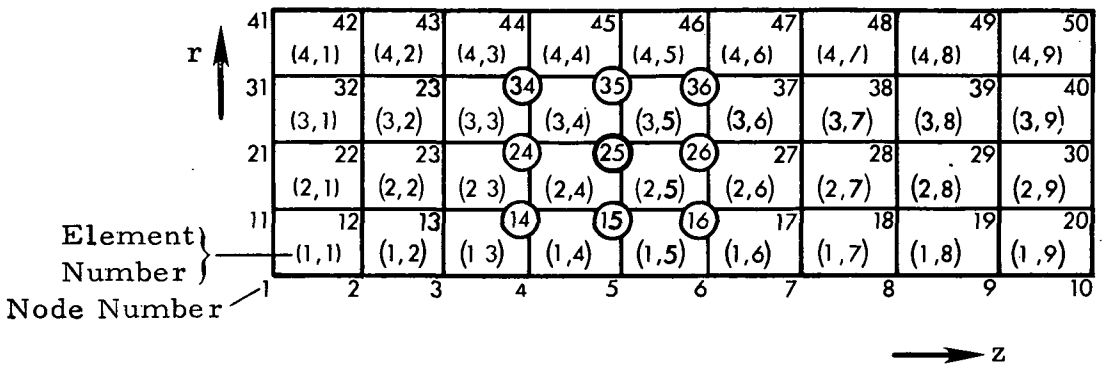

(b) Nonuniform Rectangular

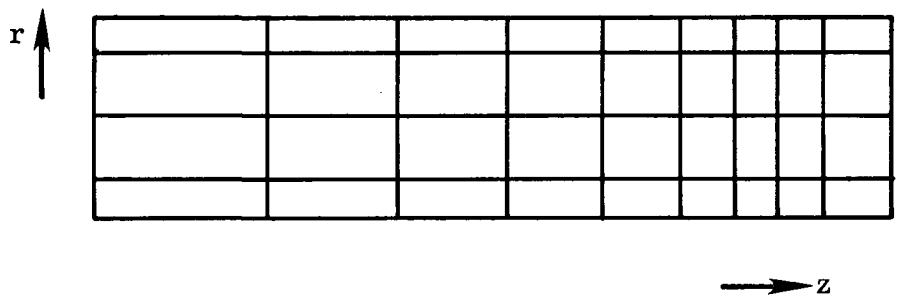

(c) Nonuniform Rectangular Mapped by a Coordinate Transformation

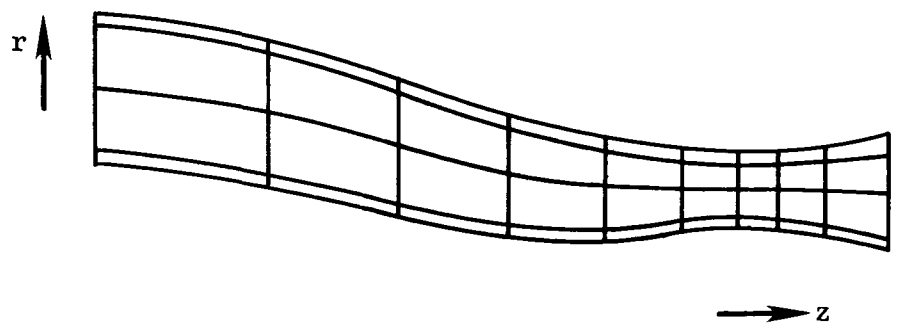

Figure 3. Rectangular Discretization in a Plane.

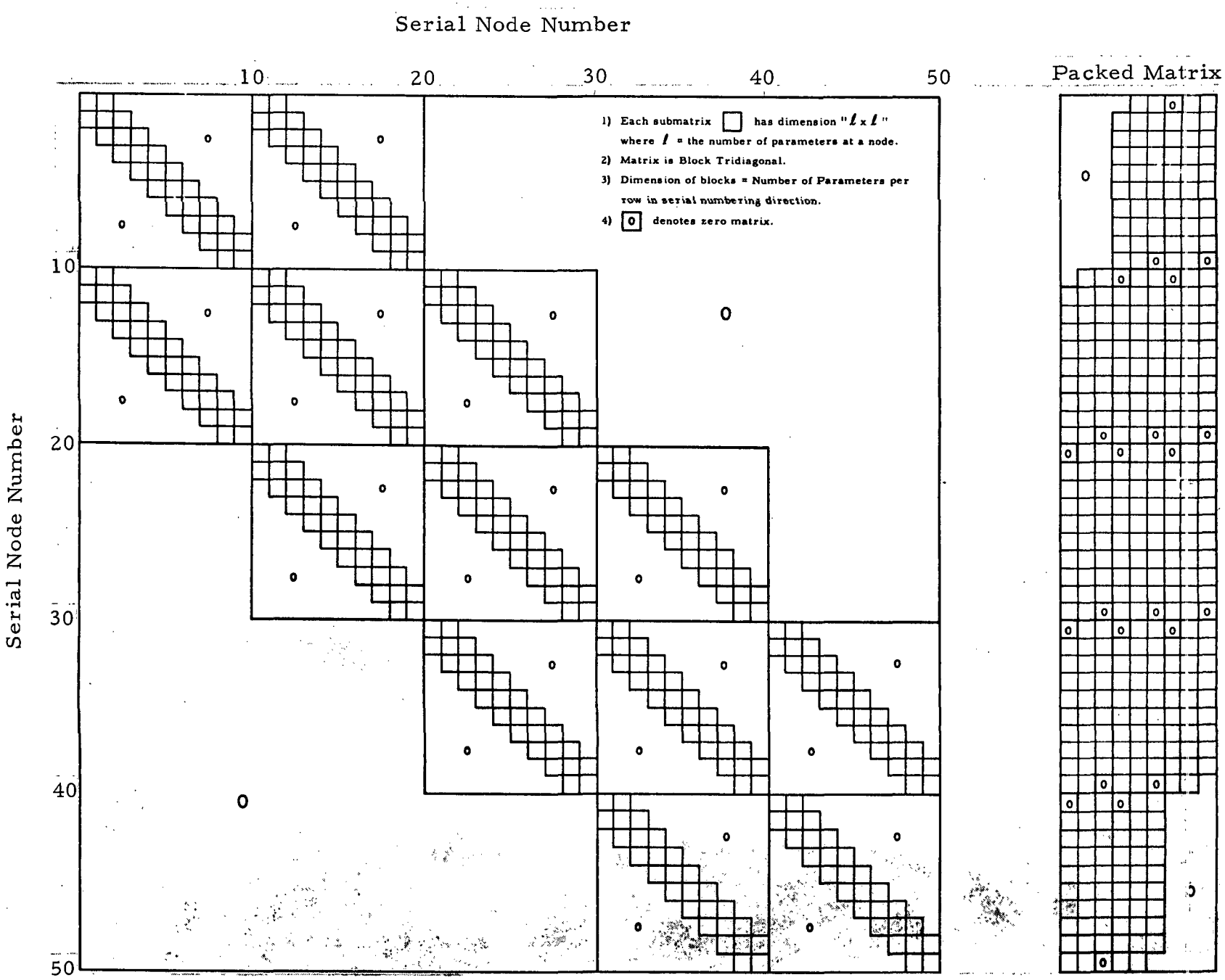

Figure 4. Matrix Map of the 2-D Rectangular Discretization of Figure 3

solution, consider whether much practical importance arises from this fact. The uniform rectangular discretization scheme from which this matrix was generated is hardly applicable to realistic problems. As shown in Figures 3(b) and 3(c), however, the identical matrix map is also generated by a nonuniform rectangular discretization, as well as by arbitrary two-dimensional mappings of the discretization grid, provided no fold-over occurs.

Solution of equations (17) through (20) may be greatly facilitated by limiting the analysis to use of this discretization scheme. The specific map for this scheme may thus be incorporated implicitly into the computer program which enables us to disregard the general but somewhat ponderous sparse matrix pointer technology. All computation and storage is thus performed implicitly only with nonzero values. In addition, this discretization scheme yields a block tridiagonal matrix of block tridiagonal matrices. Special numerical techniques, which are discussed later (section 2.8), exist for solution of matrix equations involving tridiagonal matrices.

2.3 Element Derivation

Consider the region of space enclosed by the element shown in Figure 2. Suppose that within this region the acoustic variables u, v, w, p as well as the mean fluid parameters $\bar{\rho}, \bar{U}, \bar{V}, c$ of equations (17) through (20) are defined by relations of the following type

$$u = (N_1, N_2, N_3, N_4) \begin{Bmatrix} u_1 \\ u_2 \\ u_3 \\ u_4 \end{Bmatrix} = (N)\{u\} \tag{21}$$

where u_1, u_2, u_3, u_4 are the values of " u " at the four node points at the numbered corners of the element.

Define a set of local coordinates (η, ξ) within the region such that the coordinate of the nodes (η_i, ξ_i) are given by (-1, -1), (+1, -1), (+1, +1), (-1, +1) for i = 1 through 4 respectively. The N_i's of equation (21) for the linear Serendipity element are then defined by

$$N_i = \frac{1}{4}(1 + \xi\,\xi_i)(1 + \eta\,\eta_i) \tag{22}$$

For the undeformed element shown in Figure 2, the transformation from local to global coordinates is simply

$$\eta = \frac{(r - r_c)}{b}$$
$$\xi = \frac{(z - z_c)}{a} \tag{23}$$

where (r_c, z_c) are the global coordinates of the center of the element. However, as illustrated in Figure 3, we require to map this simple shape to conform to complicated boundaries so that it then appears as shown in

Figure 5. Suppose then, that instead of equation (23) we have the transformation

$$r = (N_1, N_2, N_3, N_4) \begin{Bmatrix} r_1 \\ r_2 \\ r_3 \\ r_4 \end{Bmatrix} = (N)\{r\}$$

$$z = (N_1, N_2, N_3, N_4) \begin{Bmatrix} z_1 \\ z_2 \\ z_3 \\ z_4 \end{Bmatrix} = (N)\{z\} \qquad (24)$$

Note that in comparing these relationships with those of equation (21) two conditions are satisfied:

- The same points (viz. the node points) define the geometry and the finite element analysis points.
- The shape functions (viz. the N_i's) defining the global coordinates and the variables within the element are the same.

Thus, the mapped elements are isoparametric.

In order to transform equations (17) through (20) into the local coordinate system, we need to derive expressions for $\frac{\partial}{\partial r}$ and $\frac{\partial}{\partial z}$ in the local system

$$\frac{\partial N_i}{\partial \eta} = \frac{\partial N_i}{\partial r}\frac{\partial r}{\partial \eta} + \frac{\partial N_i}{\partial z}\frac{\partial z}{\partial \eta}$$

$$\frac{\partial N_i}{\partial \xi} = \frac{\partial N_i}{\partial r}\frac{\partial r}{\partial \xi} + \frac{\partial N_i}{\partial z}\frac{\partial z}{\partial \xi}$$

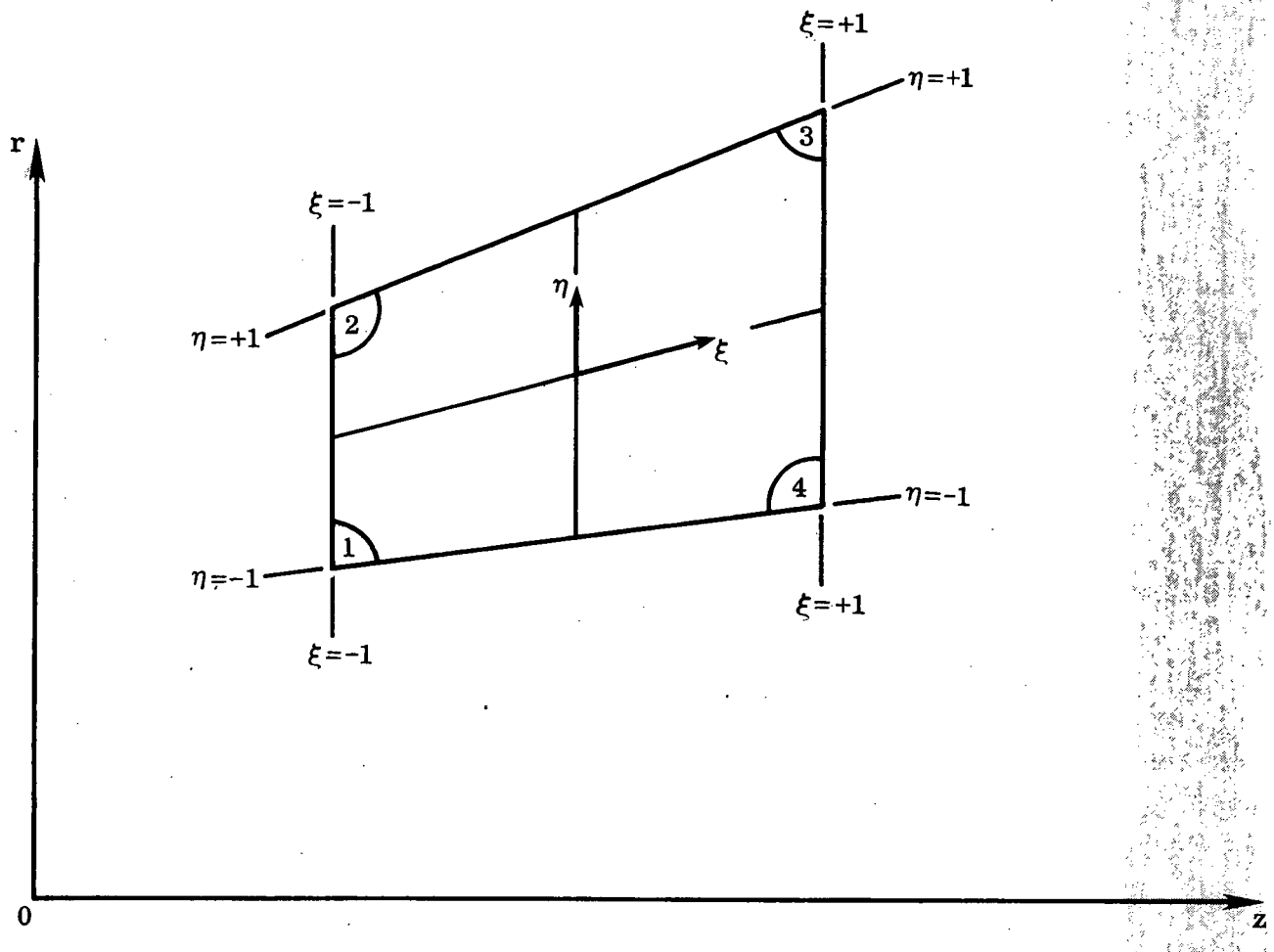

Figure 5. Deformed Element.

$$\begin{Bmatrix} \frac{\partial N_i}{\partial \eta} \\ \frac{\partial N_i}{\partial \xi} \end{Bmatrix} = \begin{bmatrix} \frac{\partial r}{\partial \eta} & \frac{\partial z}{\partial \eta} \\ \frac{\partial r}{\partial \xi} & \frac{\partial z}{\partial \xi} \end{bmatrix} \begin{Bmatrix} \frac{\partial N_i}{\partial r} \\ \frac{\partial N_i}{\partial z} \end{Bmatrix}$$

$$= [J] \begin{Bmatrix} \frac{\partial N_i}{\partial r} \\ \frac{\partial N_i}{\partial z} \end{Bmatrix} \tag{25}$$

where $[J]$ is the Jacobian Matrix.

We may thus define the matrix

$$\begin{Bmatrix} (\alpha_r) \\ (\alpha_z) \end{Bmatrix} = \begin{Bmatrix} \frac{\partial}{\partial r}(N) \\ \frac{\partial}{\partial z}(N) \end{Bmatrix}$$

$$= [J]^{-1} \begin{Bmatrix} \frac{\partial}{\partial \eta}(N) \\ \frac{\partial}{\partial \xi}(N) \end{Bmatrix} \tag{26}$$

Suppose equations (21), (24) and (26) are substituted into equations (17) through (20). Using the Galerkin version of the method of weighted residuals, we wish to integrate over the element, weighting each equation in turn by each of the N_i's to obtain the following four matrix equations in the nodal variables. It is convenient in integrating these equations to do so in the local, rather than in the global, coordinate system because this greatly simplifies the process due to the convenient limits of integration. Effectively, integration is then over the simple shape of Figure 2, rather than the complicated, distorted shape of Figure 5. In order to perform this operation, it is necessary to determine an expression for an element of area (dA) in the local system. It is shown in Appendix 1, that "dA" is given by

$$dA = |J|\, d\eta\, d\xi \tag{27}$$

where $|J|$ is the determinant of the Jacobian matrix. Equations (17) through (20) thus become:

$$\int_0^{2\pi}\int_{-1}^{+1}\int_{-1}^{+1} (N)\{r\}\{N\}\Big(\Big[\omega + (\alpha_z)\{\bar{u}\}\Big](N) + (N)\{\bar{V}\}(\alpha_r) + (N)\{\bar{u}\}(\alpha_z),$$

$$(\alpha_r)\{\bar{u}\}(N),\ 0,\ \frac{1}{(N)\{\bar{\rho}\}}\left[\left[\frac{(\alpha_r)\{\bar{u}\}(N)\{\bar{V}\} + (N)\{\bar{u}\}(\alpha_z)\{\bar{u}\}}{[(N)\{c\}]^2}\right](N)\right.$$

$$\left.+ (\alpha_z)\right]\Big)\begin{Bmatrix}\{u\}\\ \{v\}\\ \{w\}\\ \{p\}\end{Bmatrix}|J|\, d\eta\, d\xi\, d\theta = 0 \tag{28}$$

$$\int_0^{2\pi}\int_{-1}^{+1}\int_{-1}^{+1} (N)\{r\}\{N\}\Big((\alpha_z)\{\bar{V}\}(N),\Big[\omega + (\alpha_r)\{\bar{V}\}\Big](N) + (N)\{\bar{V}\}(\alpha_r)$$

$$+ (N)\{\bar{u}\}(\alpha_z),\ 0,\ \frac{1}{(N)\{\bar{\rho}\}}\left[\left[\frac{(N)\{\bar{V}\}(\alpha_r)\{\bar{V}\} + (N)\{\bar{u}\}(\alpha_z)\{\bar{V}\}}{[(N)\{c\}]^2}\right](N)\right.$$

$$\left.+ (\alpha_r)\right]\Big)\begin{Bmatrix}\{u\}\\ \{v\}\\ \{w\}\\ \{p\}\end{Bmatrix}|J|\, d\eta\, d\xi\, d\theta = 0 \tag{29}$$

$$\int_{0}^{2\pi}\int_{-1}^{+1}\int_{-1}^{+1} (N)\{r\}\{N\}\left(0\ ,\ 0\ ,\ \left[\omega + \frac{(N)\{\bar{V}\}}{(N)\{r\}}\right](N) + (N)\{\bar{V}\}(\alpha_r) \right.$$

$$\left. + (N)\{\bar{U}\}(\alpha_z)\ ,\ \frac{m}{(N)\{r\}\,(N)\{\bar{S}\}}(N)\right) \begin{Bmatrix}\{u\}\\ \{v\}\\ \{w\}\\ \{p\}\end{Bmatrix} |J|\, d\eta\, d\xi\, d\theta = 0 \qquad (30)$$

$$\int_{0}^{2\pi}\int_{-1}^{+1}\int_{-1}^{+1} (N)\{r\}\{N\}\left((\alpha_z)\{\bar{S}\}(N) + (N)\{\bar{S}\}(\alpha_z)\ ,\ \left[(\alpha_r)\{\bar{S}\} + \frac{(N)\{\bar{S}\}}{(N)\{r\}}\right](N) \right.$$

$$+ (N)\{\bar{S}\}(\alpha_r)\ ,\ \frac{m\,(N)\{\bar{S}\}\,(N)}{(N)\{r\}}\ ,\ \frac{1}{[(N)\{c\}]^2}\left[\left[(\alpha_z)\{\bar{U}\} + (\alpha_r)\{\bar{V}\}\right.\right.$$

$$\left. + \frac{(N)\{\bar{V}\}}{(N)\{r\}} + \omega - \frac{2}{(N)\{c\}}\left[(N)\{\bar{U}\}(\alpha_z)\{c\} + (N)\{\bar{V}\}(\alpha_r)\{c\}\right]\right](N)$$

$$\left. + (N)\{\bar{U}\}(\alpha_z) + (N)\{\bar{V}\}(\alpha_r)\right]\ \Big)\ \begin{Bmatrix}\{u\}\\ \{v\}\\ \{w\}\\ \{p\}\end{Bmatrix} |J|\, d\eta\, d\xi\, d\theta = 0 \qquad (31)$$

2.4 Algebraic Integration for Ducts of Constant Cross-Sectional Area

If we assume that we are dealing only with ducts of constant cross-section and that

- the mean flow is incompressible,
- there is no mean flow in the radial direction,
- the mean axial flow has no gradient in the axial direction.

Equations (17) through (20) now become

$$ku + M'v + M\frac{\partial u}{\partial z} + \frac{1}{\varepsilon}\frac{\partial p}{\partial z} = 0 \tag{32}$$

$$kv + M\frac{\partial v}{\partial z} + \frac{1}{\varepsilon}\frac{\partial p}{\partial r} = 0 \tag{33}$$

$$kw + M\frac{\partial w}{\partial z} + \frac{m}{\varepsilon r}p = 0 \tag{34}$$

$$kp + M\frac{\partial p}{\partial z} + \varepsilon\left\{\frac{\partial u}{\partial z} + \frac{\partial v}{\partial r} + \frac{1}{r}(v + mw)\right\} = 0 \tag{35}$$

where

$$M = \frac{\bar{u}}{c} \tag{36}$$

$$M' = \frac{1}{c}\frac{\partial \bar{u}}{\partial c} \tag{37}$$

$$\varepsilon = \bar{\rho} c \tag{38}$$

From equation (23), we have that

$$\begin{aligned} r &= b\eta + r_c \\ z &= a\xi + z_c \end{aligned} \tag{39}$$

whence it follows that

$$\begin{aligned} dr &= b\,d\eta \\ dz &= a\,d\xi \end{aligned} \tag{40}$$

Supposing a linear dependence for M within each element,

$$M = M_c + M'(r - r_c)$$

$$= M_c + M' b \eta$$

We may integrate over the element using the Galerkin procedure as in section 2.3 (note that now $|J|$, the determinant of the Jacobian, is unity)

$$\int_0^{2\pi}\int_{-1}^{1}\int_{-1}^{1} (b\eta + r_c)\, N_i \left[k u + v M' + \frac{(M_c + M' b\eta)}{a} \frac{\partial u}{\partial \xi} + \frac{1}{\varepsilon a} \frac{\partial p}{\partial \xi} \right] d\xi\, d\eta\, d\theta = 0 \tag{41}$$

$$\int_0^{2\pi}\int_{-1}^{1}\int_{-1}^{1} (b\eta + r_c)\, N_i \left[k v + \frac{(M_c + M' b\eta)}{a} \frac{\partial v}{\partial \xi} + \frac{1}{\varepsilon b} \frac{\partial p}{\partial \xi} \right] d\xi\, d\eta\, d\theta = 0 \tag{42}$$

$$\int_0^{2\pi}\int_{-1}^{1}\int_{-1}^{1} (b\eta + r_c)\, N_i \left[k w + \frac{(M_c + M' b\eta)}{a} \frac{\partial w}{\partial \xi} + \frac{m p}{\varepsilon (b\eta + r_c)} \right] d\xi\, d\eta\, d\theta = 0 \tag{43}$$

$$\int_0^{2\pi}\int_{-1}^{1}\int_{-1}^{1} (b\eta + r_c)\, N_i \left[k p + \frac{(M_c + M' b\eta)}{a} \frac{\partial p}{\partial \xi} + \varepsilon \left(\frac{1}{a} \frac{\partial u}{\partial \xi} + \frac{1}{b} \frac{\partial v}{\partial \eta} + \frac{(v + m w)}{(b\eta + r_c)} \right) \right] \cdot d\xi\, d\eta\, d\theta = 0 \tag{44}$$

where (i = 1 to 4) yielding a total of sixteen equations. Writing u, v, w and p in terms of the nodal coordinates as in equation (21)

$$u = (N)\{u\} \qquad w = (N)\{w\}$$

$$v = (N)\{v\} \qquad p = (N)\{p\} \tag{45}$$

equations (41) through (44) may readily be integrated.

Before performing these integrations, however, let us consider how conditions at the element boundaries may affect the integration. If equations (32) through (35) contained second-order terms it would be necessary to integrate these by parts to reduce them to first order since second-order terms require continuity of first-order terms over a boundary (Ref. 18, page 42). However, using a linear element with a linear system of equations has advantages in this respect since we only need to satisfy the requirement of continuity of the variables themselves across boundaries. Also, along the outer boundary, it is sufficient to constrain the appropriate variables to conform to the boundary conditions without the necessity of evaluating the specific boundary integral.

Equations (41) through (44) become

$$\left(k[\alpha] + [\beta],\ M'[\alpha],\ 0,\ \frac{1}{\varepsilon}[\gamma]\right)\begin{Bmatrix}\{u\}\\ \{v\}\\ \{w\}\\ \{p\}\end{Bmatrix} = 0 \tag{46}$$

$$\left(0,\ k[\alpha] + [\beta],\ 0,\ \frac{1}{\varepsilon}[\mu]\right)\begin{Bmatrix}\{u\}\\ \{v\}\\ \{w\}\\ \{p\}\end{Bmatrix} = 0 \tag{47}$$

$$\left(0,\ 0,\ k[\alpha] + [\beta],\ \frac{m}{\varepsilon}[\delta]\right)\begin{Bmatrix}\{u\}\\ \{v\}\\ \{w\}\\ \{p\}\end{Bmatrix} = 0 \tag{48}$$

$$\left(\varepsilon[\gamma],\ \varepsilon\left[[\mu] + [\delta]\right],\ m\varepsilon[\delta],\ k[\alpha] + [\beta]\right)\begin{Bmatrix}\{u\}\\ \{v\}\\ \{w\}\\ \{p\}\end{Bmatrix} = 0 \tag{49}$$

where $[\alpha]$, $[\beta]$, $[\gamma]$, $[\delta]$ and $[\mu]$ are defined in appendix 2.

2.5 Numerical Integration for Arbitrary Axisymmetric Ducts

Numerical integration of equations (28) through (31) by a standard integration formula is a trivial procedure in concept. However, because of the necessity to integrate a large number of elements in this manner, consider the equations more carefully and optimize the process.

Since none of the variables is an explicit function of " θ ", the integration with respect to " θ " results simply in a multiplicative constant of 2 which may be ignored.

It may be seen that many coefficients of the matrix equations are multiplied by scalar quantities. These are defined below:

$$
\begin{aligned}
A &= (N)\{r\} & B &= (N)\{\bar{\rho}\} \\
C &= (N)\{\bar{V}\} & D &= (N)\{\bar{U}\} \\
E &= (\alpha_r)\{\bar{V}\} & F &= (\alpha_z)\{\bar{V}\} \\
G &= (\alpha_r)\{\bar{U}\} & H &= (\alpha_z)\{\bar{U}\} \\
I &= (\alpha_r)\{\bar{\rho}\} & L &= (\alpha_r)\{c\} \\
K &= (N)\{c\} & Q &= (\alpha_z)\{\bar{\rho}\} \\
M &= (\alpha_z)\{c\}
\end{aligned}
\qquad (50)
$$

where the quantities A through Q are functions of ξ and η.

Substituting in equations (28) to (31) we get

$$
\int_{-1}^{1}\int_{-1}^{1} A\{N\}\left([\omega + H](N) + C(\alpha_r) + D(\alpha_z),\ G(N),\ 0,\ \frac{1}{B}\left[\left[\frac{GC + DH}{K^2}\right](N) + (\alpha_z)\right]\right)\begin{Bmatrix}\{u\}\\ \{v\}\\ \{w\}\\ \{p\}\end{Bmatrix} \cdot |J|\, d\eta\, d\xi = 0 \qquad (51)
$$

$$\int_{-1}^{1}\int_{-1}^{1} A\{N\}\left(F(N),\ [\omega + E](N) + C(\alpha_r) + D(\alpha_z),\ 0,\ \frac{1}{B}\left[\left[\frac{CE+DF}{K^2}\right](N) + (\alpha_r)\right]\right)\begin{Bmatrix}\{u\}\\ \{v\}\\ \{w\}\\ \{p\}\end{Bmatrix} \cdot |J|\, d\eta\, d\xi = 0 \qquad (52)$$

$$\int_{-1}^{1}\int_{-1}^{1} A\{N\}\left(0,\ 0,\ \left[\omega + \frac{C}{A}\right](N) + C(\alpha_r) + D(\alpha_z),\ \frac{m}{AB}(N)\right)\begin{Bmatrix}\{u\}\\ \{v\}\\ \{w\}\\ \{p\}\end{Bmatrix} \cdot |J|\, d\eta\, d\xi = 0 \qquad (53)$$

$$\int_{-1}^{1}\int_{-1}^{1} A\{N\}\left(Q(N) + B(\alpha_z),\ \left[I + \frac{B}{A}\right](N) + B(\alpha_r),\ \frac{mB}{A}(N),\right.$$
$$\left.\frac{1}{K^2}\left[\left[H + E + \frac{C}{A} + \omega - \frac{2}{K}[DM + CL]\right](N) + C(\alpha_r)\right]\right)\begin{Bmatrix}\{u\}\\ \{v\}\\ \{w\}\\ \{p\}\end{Bmatrix} |J|\, d\eta\, d\xi = 0 \qquad (54)$$

The Gaussian quadrature procedure that is used employs unevenly spaced abscissa points (η_i, ξ_i). The corresponding weights to be applied at these points (H_i, H_i'). If we choose the same number of points (n_G) in each direction, then $\eta_i = \xi_i$ and $H_i = H_i'$. Thus,

$$I = \int_{-1}^{1}\int_{-1}^{1} f(\xi, \eta)\, d\xi\, d\eta$$

$$= \int_{-1}^{1} \left(\sum_{j=1}^{n_G} H_j\, f(\xi_j, \eta) \right) d\eta$$

$$= \sum_{i=1}^{n_G} \sum_{j=1}^{n_G} H_i\, H_j\, f(\xi_j, \eta_i) \qquad (55)$$

Tables of abscissae and weights for different values of n_G are given in [18] and are reproduced in Appendix 3.

The logic diagram for evaluation of equations (51) through (54) using equation (55) is shown in Figure 6. It may be seen that it is possible to retain several potentially time-consuming steps outside the innermost loops of the quadrature process.

2.6 Global Matrix Assembly, Packing Technique, and Insertion of Boundary Conditions

Assembly of a global matrix equation, that is, a matrix equation representing the entire system, from a set of finite element matrix equations is basic procedure in the finite element technique, e.g., reference 18, page 13, and is not described in detail. From Figure 3(a), it may be seen, however, that there is a one-to-one correspondence between the global serial numbering system of nodes and the element numbering system together with its local node numbering as shown in Figure 2. Appropriate shifting of rows and columns are all that is required to add the local element matrix directly into the global matrix.

This procedure is somewhat complicated by the fact that when a global matrix possesses a map as that shown in Figure 4, it is undesirable to store anything but the three diagonal bands of nonzero coefficients. The most convenient way to "pack" a matrix of this form is shown to the right of the full or expanded matrix in Figure 4, where the diagonal bands are arranged in vertical columns. The algorithm to yield a column number in the packed matrix from a row and column number in the expanded matrix is listed in Appendix 4.

Along the outer boundaries of the discretised region, two kinds of boundary

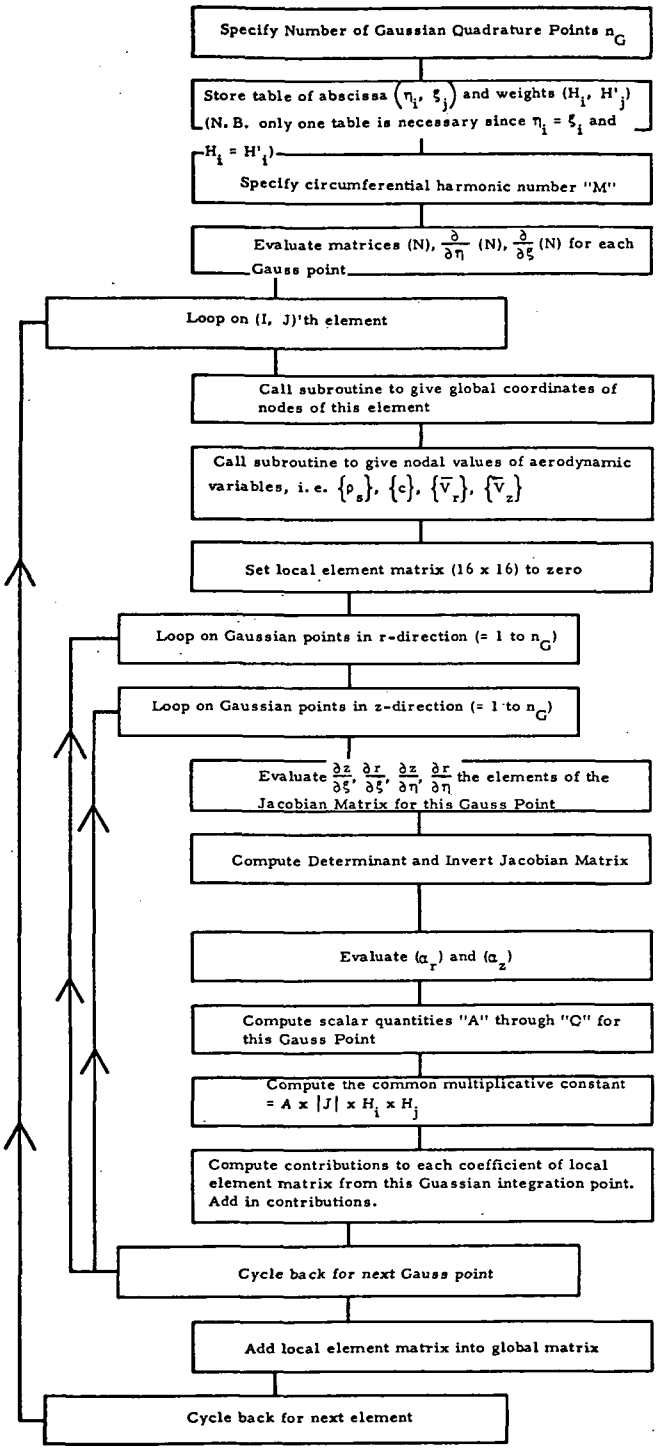

Figure 6. Logic Diagram for Evaluation of Integrals.

conditions may exist, noise source or admittance. The boundary condition at the radiation plane may be forced to conform to an admittance boundary condition as shown in Appendix 5.

Provision is made for insertion of the two kinds of boundary condition into the assembled global matrix equation by imposing relations on the nodal variables along each boundary.

The noise source boundary condition consists simply of setting all nodal pressure coordinates equal to a specified constant value (implying by equation (16) a specified harmonic amplitude). For example, see Appendix 6.

The admittance boundary condition involves specifying a linear relationship between nodal pressure coordinates along the boundary and the normal component of acoustic velocity. For example, see Appendix 7.

The examples in appendices 6 and 7 assume that, providing the global matrix is stored in packed form, it may be held entirely within direct access memory. This is not the case however, because by definition (see section 2.2) we will be dealing with extremely large problems employing over one hundred thousand degrees of freedom.

During assembly of the global matrix, however, it is unnecessary to have the entire matrix in direct access memory. Figures 3a and 4 show that contributions to the equations for variables at global node number 25 (for example) may only come from elements (2, 4), (2, 5), (3, 4), and (3, 5). Thus, it is only necessary to hold variables corresponding to two element rows (or three nodal rows) in direct access storage at any particular time. This is also the case for application of boundary conditions, since in Appendix 7, equation (1),

for example, X_k , X_ℓ , and X_m are all variables attributable to a single node and thus all lie within the diagonal submatrix. Suppose that their equivalents are specifically attributable to node 25 in Figure 4. The only rows and columns affected by application of the boundary conditions thus lie within the bounds of those attributable to node 25. Thus, if matrix block rows from number 11 to number 30 are in direct access memory, the boundary condition may be applied to these only with the result being identical to an application to the entire matrix.

2.7 Solution of Matrix Equation

The matrices generated by the Galerkin formulation of sections 2.4 and 2.5 are in general unsymmetric and nonpositive definite in addition to being complex. Due to the discretization scheme described in section 2.2, they are block tridiagonal.

The LU-decomposition of a block tridiagonal matrix is readily obtainable (Ref. 19, pages 166 and 173). The LU-decomposition takes the form

$$\begin{bmatrix} [a_1] & [c_1] & & & \\ [b_2] & [a_2] & [c_2] & & \\ & \ddots & \ddots & \ddots & \\ & & [a_{n-1}] & [b_{n-1}] & [c_{n-1}] \\ & & & [b_n] & [a_n] \end{bmatrix} = \begin{bmatrix} [I] & & & \\ [\beta_2] & [I] & & \\ & \ddots & \ddots & \\ & & [\beta_{n-1}] & [I] \\ & & & [\beta_n] & [I] \end{bmatrix} \begin{bmatrix} [\alpha_1] & [c_1] & & \\ & [\alpha_2] & [c_2] & \\ & & \ddots & \ddots \\ & & & [\alpha_{n-1}] & [c_n] \\ & & & & [\alpha_n] \end{bmatrix} \quad (56)$$

where $[I]$ is the identity matrix and where the two matrices on the right-hand side of the equation are the lower $[L]$ and upper $[U]$ triangular factors, respectively. The component matrices of $[L]$ and $[U]$ are given by direct substitution as

$$[\alpha_1] = [a_1] \tag{57}$$

$$[\beta_k] = [b_k]\,[\alpha_{k-1}] \qquad k = 2, n \tag{58}$$

$$[\alpha_k] = [a_k] - [\beta_k]\,[c_{k-1}] \qquad k = 2, n \tag{59}$$

The system of equations

$$[A]\{x\} = \{F\} \tag{60}$$

now becomes,

$$[L]\,[U]\{x\} = \{F\} \tag{61}$$

which decomposes into two triangular systems

$$[L]\{y\} = \{F\} \tag{62}$$

and

$$[U]\{X\} = \{Y\} \tag{63}$$

which may be solved in turn in the usual manner by forward and backward substitution using the relations

$$\{y_1\} = \{f_1\} \tag{64}$$

$$\{y_i\} = \{f_i\} - [\beta_i]\{y_{i-1}\} \qquad i = 2, n \tag{65}$$

$$\{X_n\} = [\alpha_n]^{-1}\{y_n\} \tag{66}$$

$$\{X_i\} = [\alpha_i]^{-1}(\{y_i\} - [C_i]\{X_{i+1}\}) \qquad i = n-1, 1 \tag{67}$$

The process described in equations (56) through (67) may be used to solve the global matrix equation whose derivation and assembly is described in this report. We described in section 2.6 however, that assembly of the global matrix equation may be carried out efficiently by keeping only three nodal rows of coefficients in direct access memory at any one time.

In terms of the required size of direct access memory, three nodal rows of coefficients reduces to nine packed blocks and three block vectors (e.g., see Figure 4). The respective orders of these matrix elements are:

packed blocks $m\ell \times 3\ell$

block vectors $m\ell \times 1$

where m = number nodes in serial numbering direction

ℓ = number of parameters at a node.

Thus, the total storage requirement for assembly is $(27m\ell^2 + 3m\ell)$.

For solution of the matrix equation, however, an efficient minimum requirement is three packed blocks, three block vectors, and one expanded block, giving a total storage of $(9m\ell^2 + 3m\ell + 9m^2\ell^2)$. The necessity for the storage-consuming expanded block is clear from equation (58) where it may be seen that $[\beta_k]$ is a full matrix for all $(k = 2, n)$.

Careful inspection of equations (57) through (67) shows that a number of specialized matrix handling algorithms need to be used in order to limit the requirement on the number of expanded blocks to one. These include the following:

- Transposition of either a packed or expanded matrix, and superimposing the transposed matrix upon the original storage area.
- Multiplication of an expanded matrix by a packed matrix, and superimposing the result over the storage area of the original expanded matrix.
- Addition and subtraction of expanded and packed matrices, and superimposing the result over the storage area of the original expanded matrix.
- Multiplication of a packed matrix by a vector without expanding the packed matrix.

Once the necessity for these algorithms is recognized, however, their preparation is trivial. Their use in the implementation of equations (57) through (67) together with a map of direct access storage requirements is shown in Figure 7.

2.8 Acoustic Attenuation

The principal final result of an analysis of sound propagation in an engine duct is a value for its acoustic attenuation.

Clearly from equation (16), any evaluation of the total attenuation for sources emitting sound over a broad frequency band, and with an arbitrary spatial distribution of amplitude and phase over the source plane will need to be carried out over the entire double Fourier transform implicit in this relationship. This implies practically that a value of ω has to be specified for

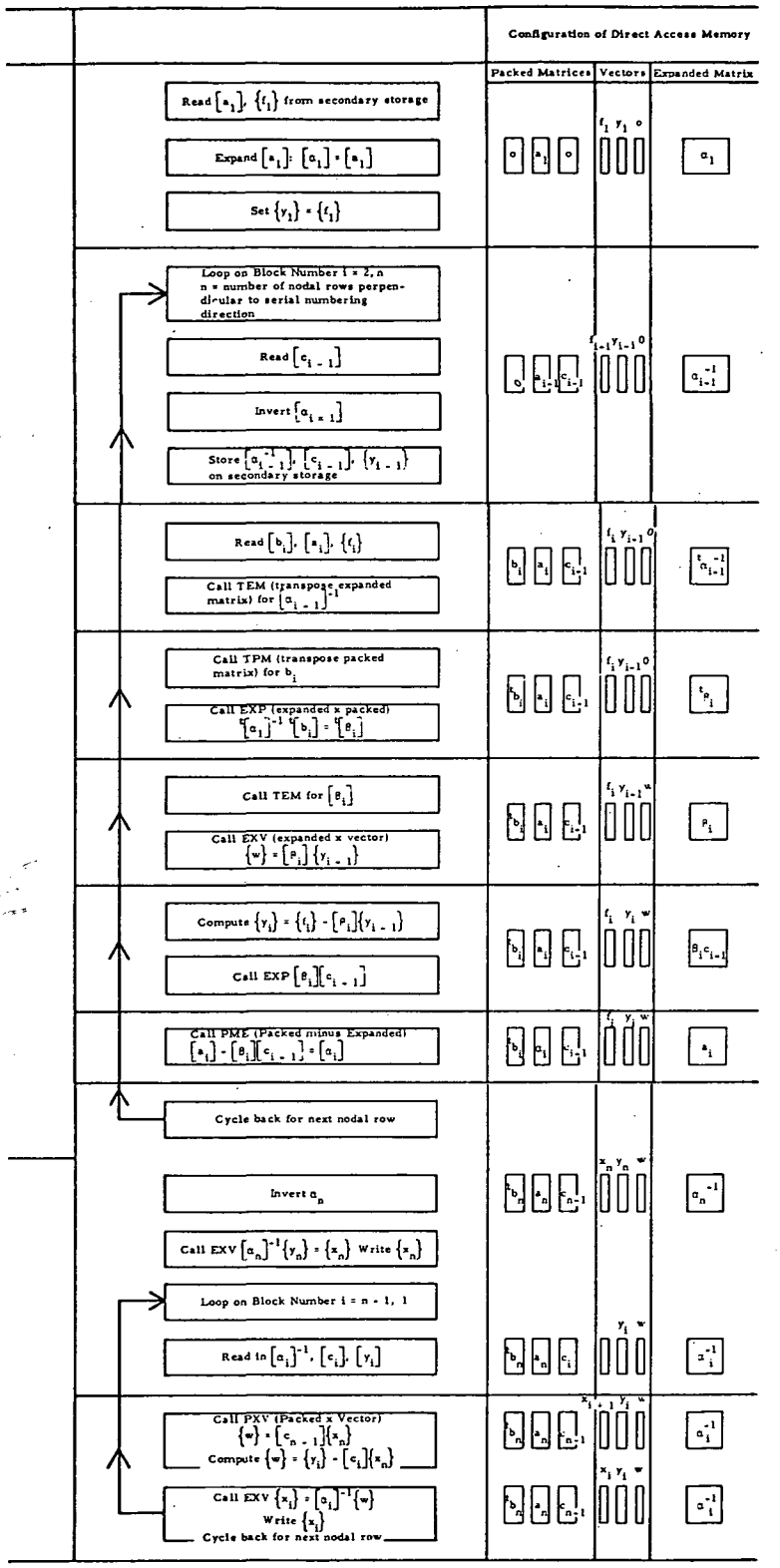

Figure 7. Description of Block Tridiagonal Matrix Solution with Memory Map.

each time harmonic, and a value of m for each angular harmonic.

Since the (ω, m) harmonics are orthogonal, acoustic intensities computed from them independently have simply to be summed to produce total intensity.

The choice of an expression for acoustic energy is not immediately clear. For irrotational, uniform-entropy flow (in the Z-direction), Cantrell and Hart[20], and Morfey[21] have shown that

$$\langle I_z \rangle = \frac{1}{2} \text{Real} \left(p u^* + M^2 p^* u + M \left(\frac{p p^*}{\bar{\rho} c} + u u^* \bar{\rho} c \right) \right) \tag{68}$$

where I_z is the axial intensity, and * denotes complex conjugate. The above expressions are accurate to second order in fluctuating quantities. However, both Cantrell and Hart, and Morfey obtained their expressions from the time-averaged energy equation. Eversman[22] used, as his starting point, the exact energy equation for a nonviscous, nonheat-conducting flow and obtained for the axial intensity:

$$\langle I_z \rangle = \frac{1}{4} \left(p u^* + p^* u \right) + \frac{M}{4} \left(\bar{\rho} c \left(u u^* + v v^* + w w^* \right) + \frac{p p^*}{\bar{\rho} c} \right) \tag{69}$$

where v - radial component of acoustic velocity

w - tangential component of acoustic velocity

Both results were programmed, with somewhat more consistent answers being obtained from the second expression. (In some instances, use of either expression results in a net increase in flux at the radiation plane over the flux at the source plane.)

In order to obtain axial acoustic flux over source F_s and radiation F_r planes, a simple linear integration scheme described in Appendix 8 was used. Duct attenuation is thus given by

$$-10 \log_{10} \left(\frac{F_r}{F_s} \right) \tag{70}$$

3.0 DESCRIPTION OF RESULTS

3.1 Comparison of Model with Previous Analyses

Comparison of the model with previous work is complicated by the fact that these comparisons can only be achieved using a small proportion of the model's total capability. These comparisons do have the advantage, however, of providing some confidence in the convergence characteristics and overall accuracy of the model.

A uniform cylindrical duct of unit radial and axial dimensions with an outer wall impedance of $\bar{\rho}c$ is shown in Figure 8. Duct attenuation was calculated at a wavenumber of unity in the absence of mean flow at a circumferential harmonic number of zero for a series of element assemblies. The solutions obtained from the model may be seen to converge on a suliton for the same problem computed from the work of Zorumski[15].

In order to verify the model's accuracy over a wide range of parameters, and to evaluate its feasibility for optimization studies, two optimization schemes were programmed. The first was a two-variable optimization to determine real and imaginary parts of a uniform liner admittance yielding maximum acoustic attenuation. This optimization was performed at two frequencies and the results are compared in Table I with those derived by Lester and Posey[23] and Quinn[24]. The results from the three analyses are substantially the same. A six-variable optimization for a three-section liner was then carried out with no significantly different results from those of Quinn. These results, together with those of Quinn, are also given in Table I.

The optimization scheme used in the two determinations above was the Davidon Fletcher Powell technique adapted to numerical gradient computations. The fact that reasonable agreement with previous analyses was

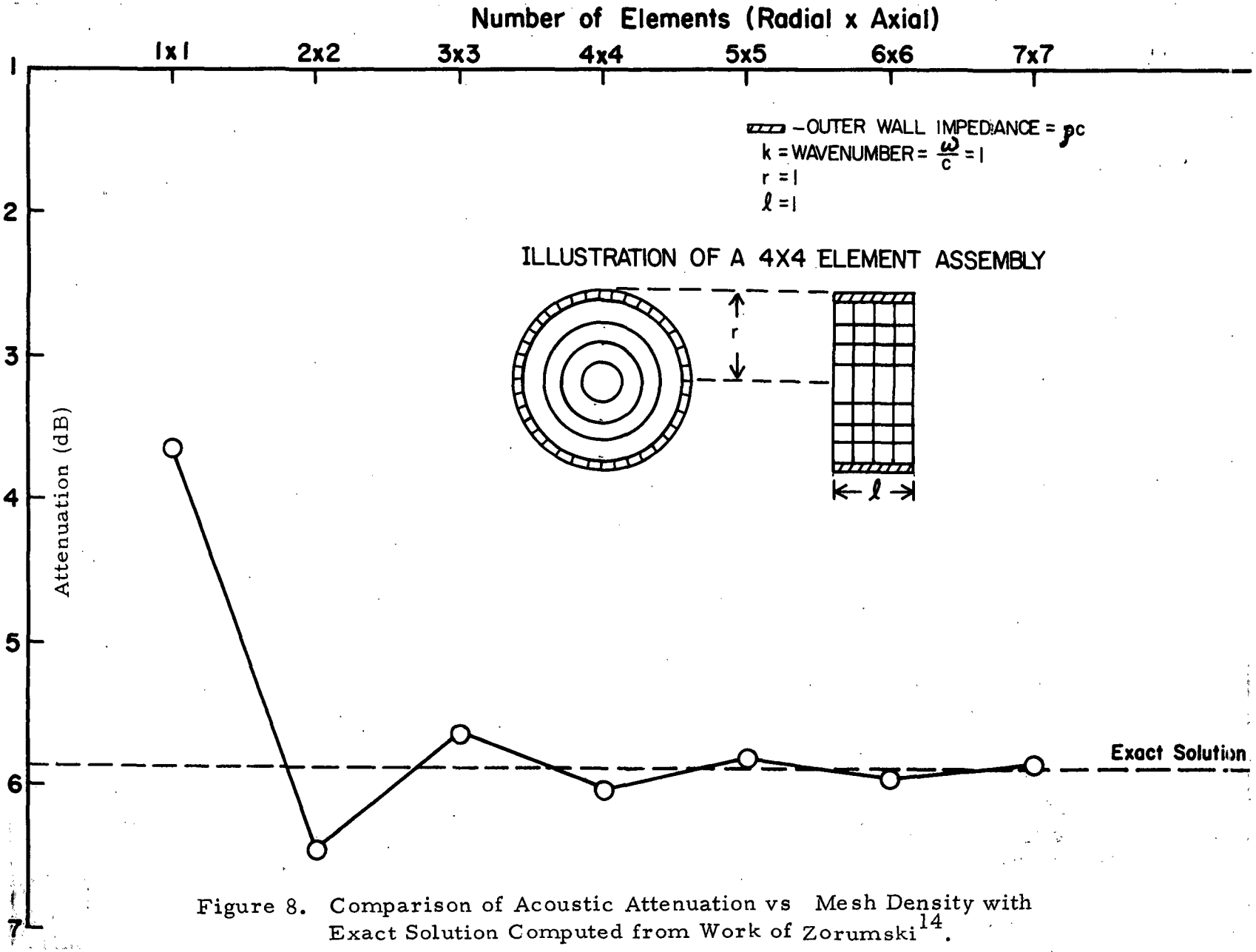

Figure 8. Comparison of Acoustic Attenuation vs Mesh Density with Exact Solution Computed from Work of Zorumski[14].

TABLE I

Comparison of Optimum Acoustic Liner Determinations

Duct radius = 1m Duct length = 2m c = 344m/sec

Circumferential wavenumber = 1, no flow

Hz	Liner Admittance (x 1/ρc)			Duct Attenuation (dB)		
	Current Analysis	Lester[23]	Quinn[24]	Current Analysis	Lester[23]	Quinn[24]
		UNIFORM LINER				
548.2	.23+ .42i	.21+ .45i	.25+ .38i	4.7	4.5	4.7
344.4	.28+ .58i	.27+ .55i	.29+ .56i	7.3	7.2	7.7
		THREE-SECTION LINER				
548.2	0+ .40i		.003+ .49i			
	.16+ .57i		.31+ .46i	6.2		7.1
	.60+ .59i		.71+ .67i			

TABLE II

Comparison of Duct Attenuations in Presence of Plug Flow

Duct radius = 1m Duct length = 2m c = 344.4m/sec

Hz	Mach No.	Circumferential Wavenumber	Liner Admittance (x 1/ρc)	Duct Attenuation (dB)	
				Current Analysis	Zorumski
54.8	-.1	0	1.46+ 1.31i	20.5	21.2
54.8	+.1	0	1.0+ 0i	10.6	10.3
274.1	+.1	1	1.0+ 0i	14.2	16.1

obtained is encouraging because evidently a sufficiently low "function noise" was present in spite of a moderately coarse analysis of 12 x 30 elements.

A conical horn was selected to verify the program for nonuniform geometry. A solution based on a small angle approximation at low frequencies is given in Morse[25]. This solution assumes a spherical wave emanating from an equivalent point source at the produced apex of the cone. The amplitude of the pressure is thus inversely proportional to the distance from this hypothetical source. Figure 9 shows the pressure variation with axial distance along a radius from the hypothetical source selected arbitrarily at 12.9° to the axis. Results from the current model (shown by a solid line) show little deviation from results produced by Morse's analysis (open circles).

A limited amount of published data is available for ducts containing flow that is suitable for comparison with the current model. In the absence of an alternative comparison, Zorumski's[15] analysis was used. This comparison is less than ideal in two ways. The current analysis is a shear-flow model, that is, the mean flow is required to go to zero at duct walls whereas Zorumski's is a plug-flow model. Further, the current model has a ρc termination impedance, whereas the version of Zorumski's model used, had a zero-reflection termination boundary condition.

Reasonable comparison is demonstrated from the results presented in Table II. For these analyses, plug flow was simulated as closely as possible in the current model by a very small shear layer. Several combinations of frequency, Mach number, circumferential harmonic wavenumber, and liner admittance are shown in Table II. No significant deviations were observed in computed duct attenuation.

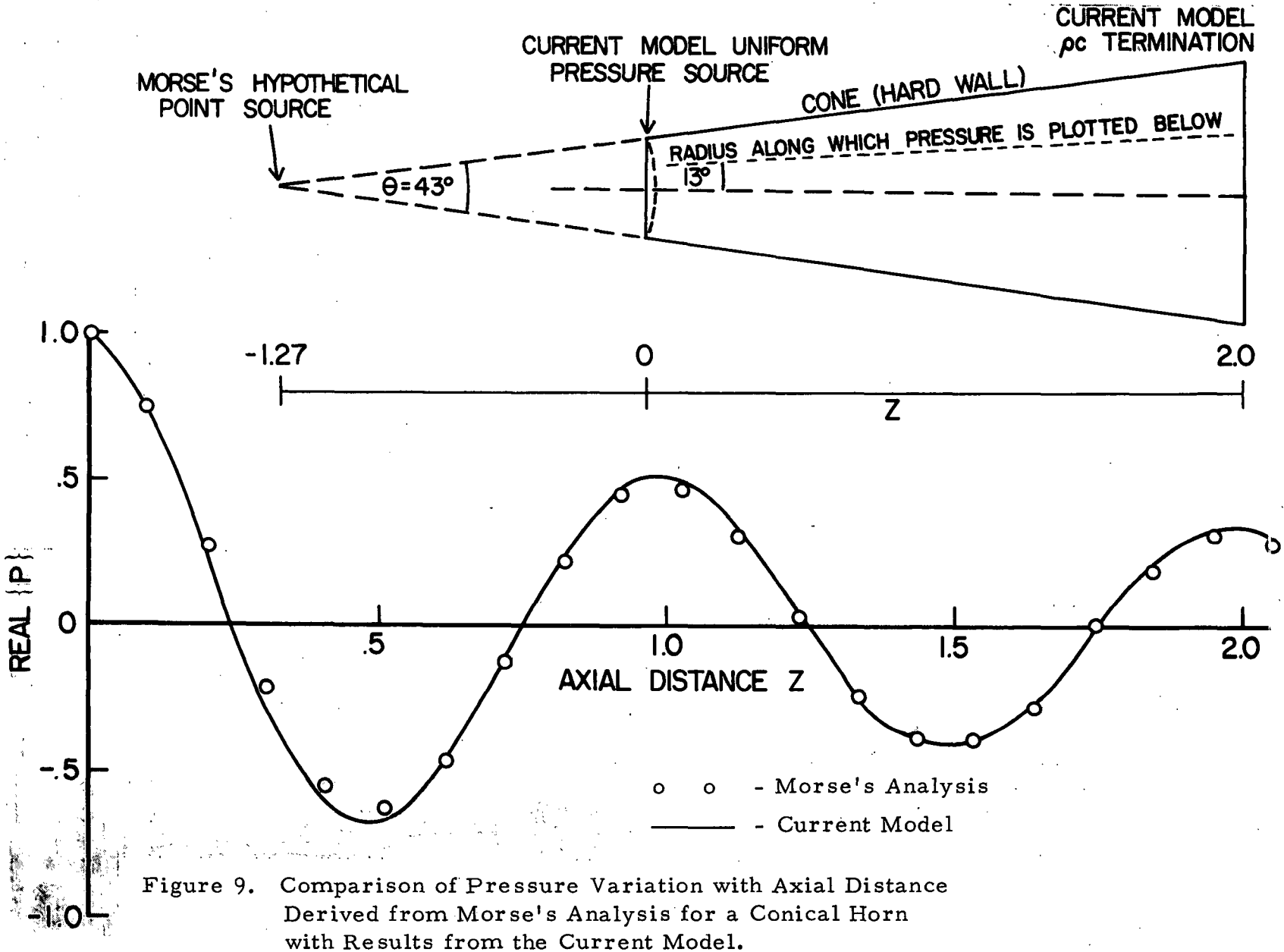

Figure 9. Comparison of Pressure Variation with Axial Distance Derived from Morse's Analysis for a Conical Horn with Results from the Current Model.

3.2 Illustrations of Potential of Current Model in Duct Optimization

The current model presents the opportunity to explore novel concepts in aero-engine duct design for optimum acoustic characteristics. This section contains illustrations of three such concepts and describes their relative success.

3.2.1 Quadratic Liner Variation

As an alternative to a sectioned liner, a uniformly varying liner is suggested. To compare directly with the three-section liner whose results are given in Table I, a quadratic liner variation was programmed. As a viable alternative in optimization studies to a three-section liner, a quadratic liner possesses the same number of variables. Its admittance β is given by

$$\beta(z) = a_o + a_1 z + a_2 z^2$$

where the a's are complex.

For the duct similar to that described in Table I, optimization coefficients yielding an admittance function given in Figure 10 was derived. Duct attenuation was 5.9 dB which compares closely with the value of 6.2 dB obtained for the three-section liner described in Table I.

3.2.2 Optimization of a Convergent-Divergent Duct

In addition to acoustic-liner parameters, the physical shape of the duct itself may be optimized for maximum acoustic attenuation. Suppose, for example, a constriction defined by a cosine function is imposed on the outer wall. The duct radius is given by

$$R = \left\{1 - q(1 - \cos 2\pi z)\right\} R_o$$

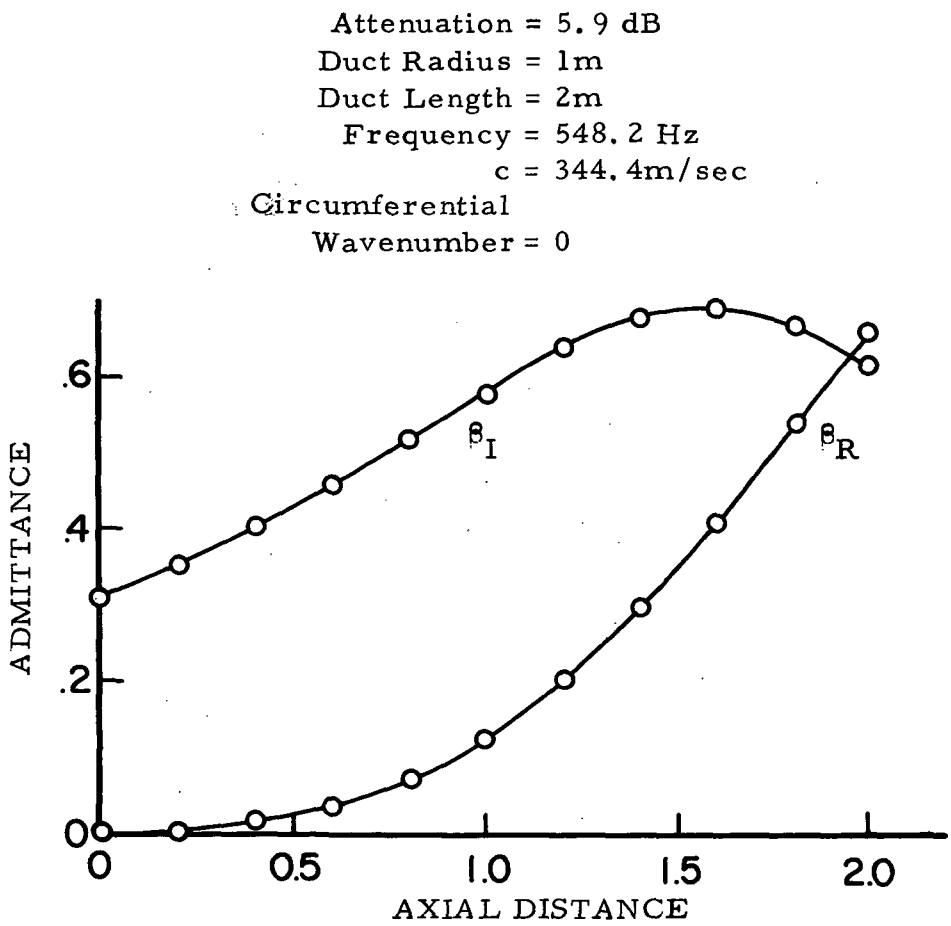

Figure 10. Admittance Variation with Axial Distance for Quadratic Liner.

where q is the constriction parameter and R_o is the duct radius at z = 0.

Suppose further that we decide to place a lower limit on the constriction size such that cross-sectional area at the throat should be no less than one-half the cross-sectional area at the source plane. Thus q should be in the range

$$0 < q < .15$$

This may be achieved by the transformation

$$q = .075(1 + \cos Q)$$

A three-variable optimization was carried out with the real and imaginary parts of a uniform admittance as variables in addition to the duct constriction parameter Q defined above.

The admittance was found to converge rapidly to the same optimum value which was previously determined for a similar duct with no constriction at the same frequency, and circumferential harmonic number. The constriction parameter, as might be expected, converged to the limiting value of

$$q = .15$$

While this exercise may seem somewhat trivial, it serves to demonstrate the possibilities of duct optimization using the model.

3.2.3 Optimization with a Center Body

The shear layer produced, as the mean flow velocity goes to zero on the walls of an aero-engine inlet duct, causes acoustic energy to be refracted

towards the duct axis is well known. This effect was verified using the model and is depicted graphically in Figure 11.

An unfortunate consequence of this effect is the decreased effectiveness of acoustic liners placed on the outer duct walls. To use an acoustically lined centerbody, such as that shown in Figure 12, shaped so as to minimize its own refraction characteristics, would appear profitable.

A three-variable optimization was carried out on a duct of this type using a cosine centerbody function similar to the function described in the previous section for a constriction. The outer duct wall was uniform (radius = 1 m), and the maximum radius of the centerbody was allowed to vary between zero and .6 of the outer wall radius. Duct length was 2 m. The other two variables in the optimization were the real and imaginary parts of the liner admittance on the centerbody and the outer wall.

A mean flow model based on streamlines, calculated on the assumption of incompressible flow, was used. Free stream velocity at the source plane was Mach .2, with a one-half sine rolloff profile. In the absence of better information, this profile was assumed to have a constant normalized shape which was independent of axial station.

At a frequency of 548.2 Hz, the centerbody radius increased to an optimum at its maximum constrained value of .6 m. The corresponding liner admittance, yielding an optimum duct attenuation of 25.8 dB, was (.62 + .38i).

This attenuation appears remarkably large when compared with the corresponding values in Table I. A partial explanation, however, is undoubtably that the dimension between the centerbody and outer duct wall is of the same order as the wavelength of the first mode.

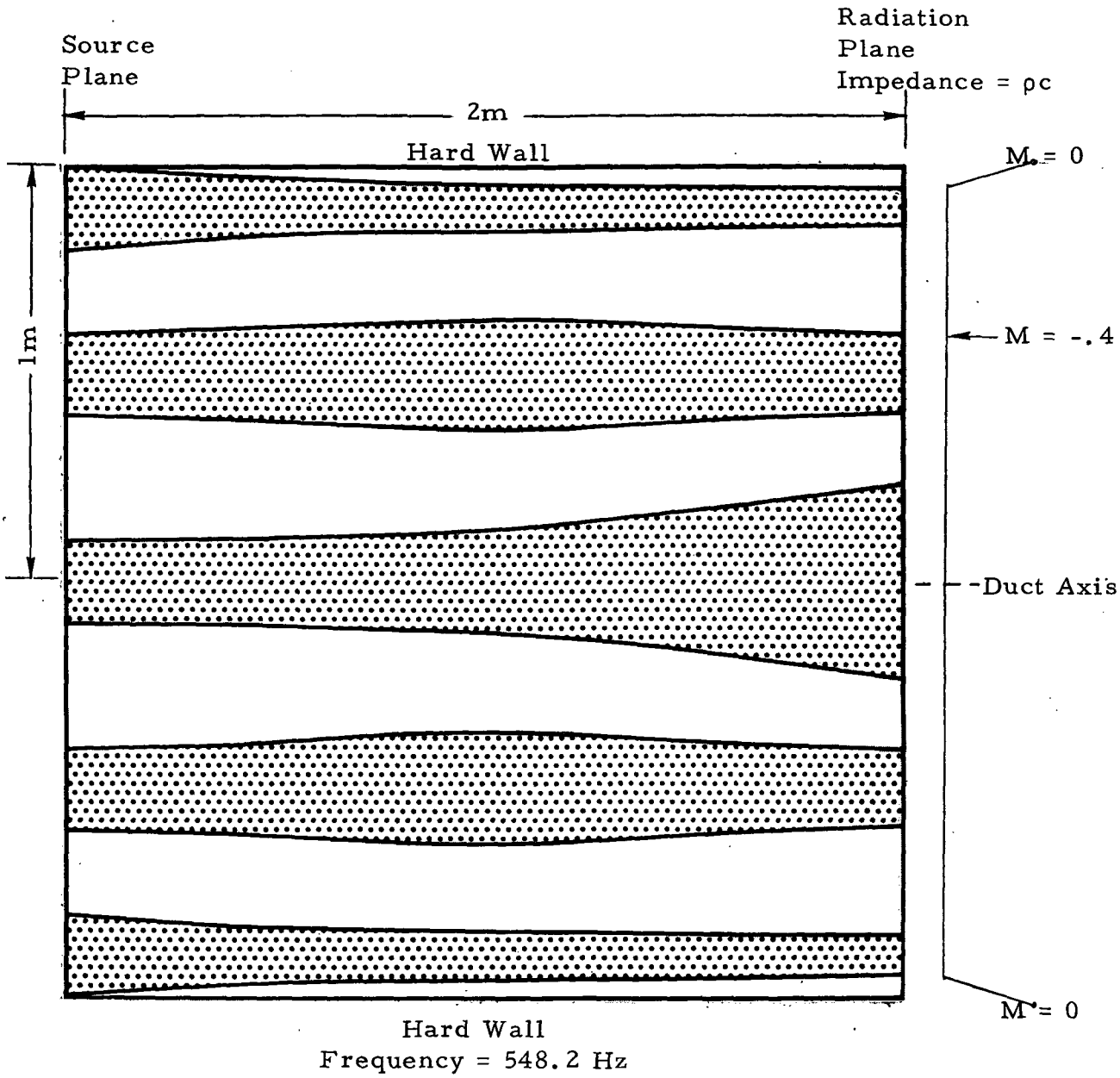

Figure 11. Plot Showing Envelopes of Pressure Amplitudes with Axial Distance at Selected Radial Stations.

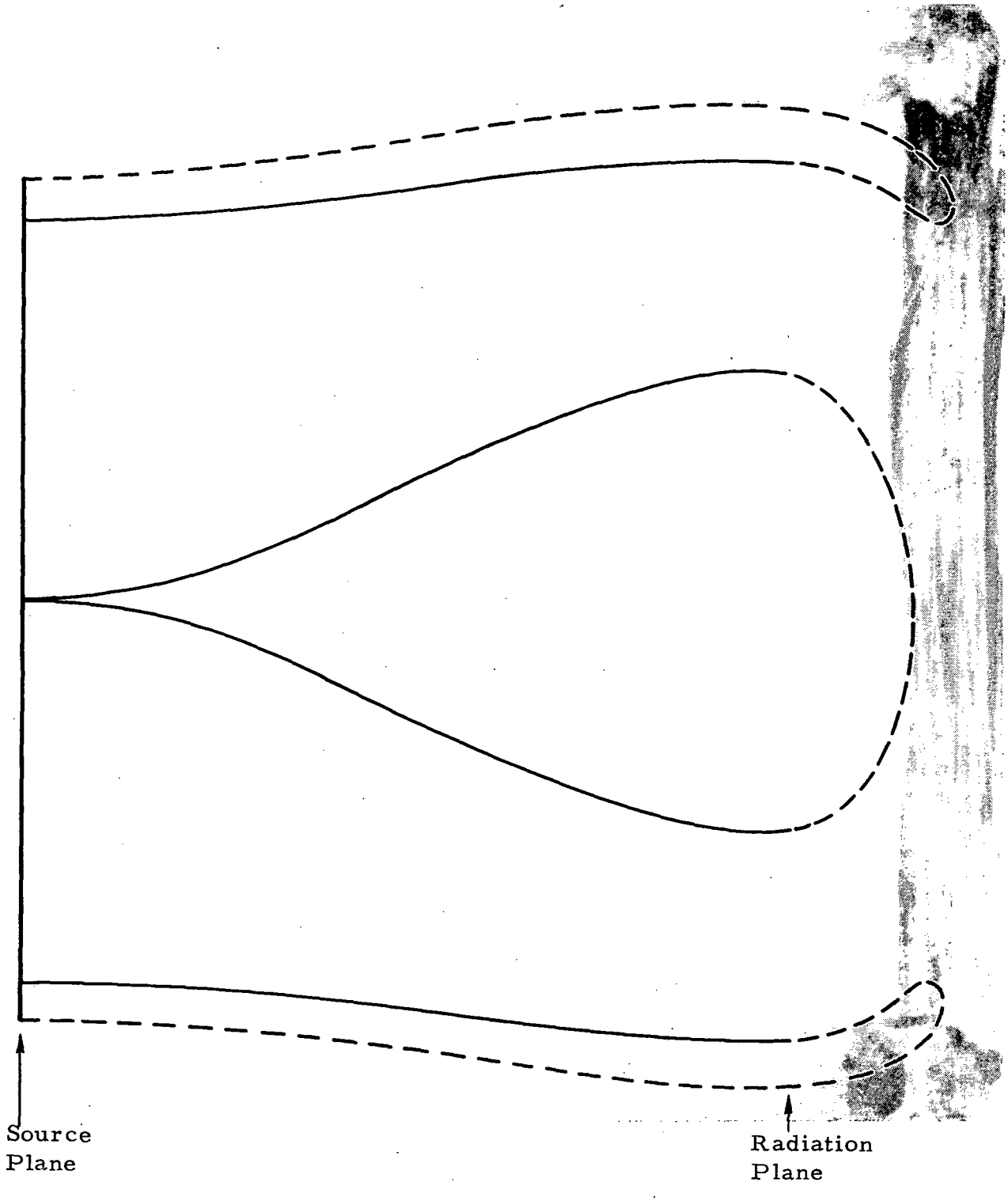

Figure 12. Constant Cross-Sectional Area Inlet Duct with Center Body.

3.3 Computing Time

The finite element model described in this report was specifically designed to operate making most efficient use of computational resources. Thus, perhaps the most important result of the study is the degree to which this objective is fulfilled.

Figure 13 shows typical central processor times that were achieved from the different variations of the model. We may draw the following conclusions from the results:

- For a particular matrix bandwidth, central processor time is roughly proportional to the matrix order.
- Numerical integration increases total computing time by roughly a factor of 1.3 over the algebraic form.

In comparison with NASTRAN (NASA Structural Analysis), the general purpose structural finite element program, the current model shows a speed improvement for similar matrices of approximately a factor of 12.

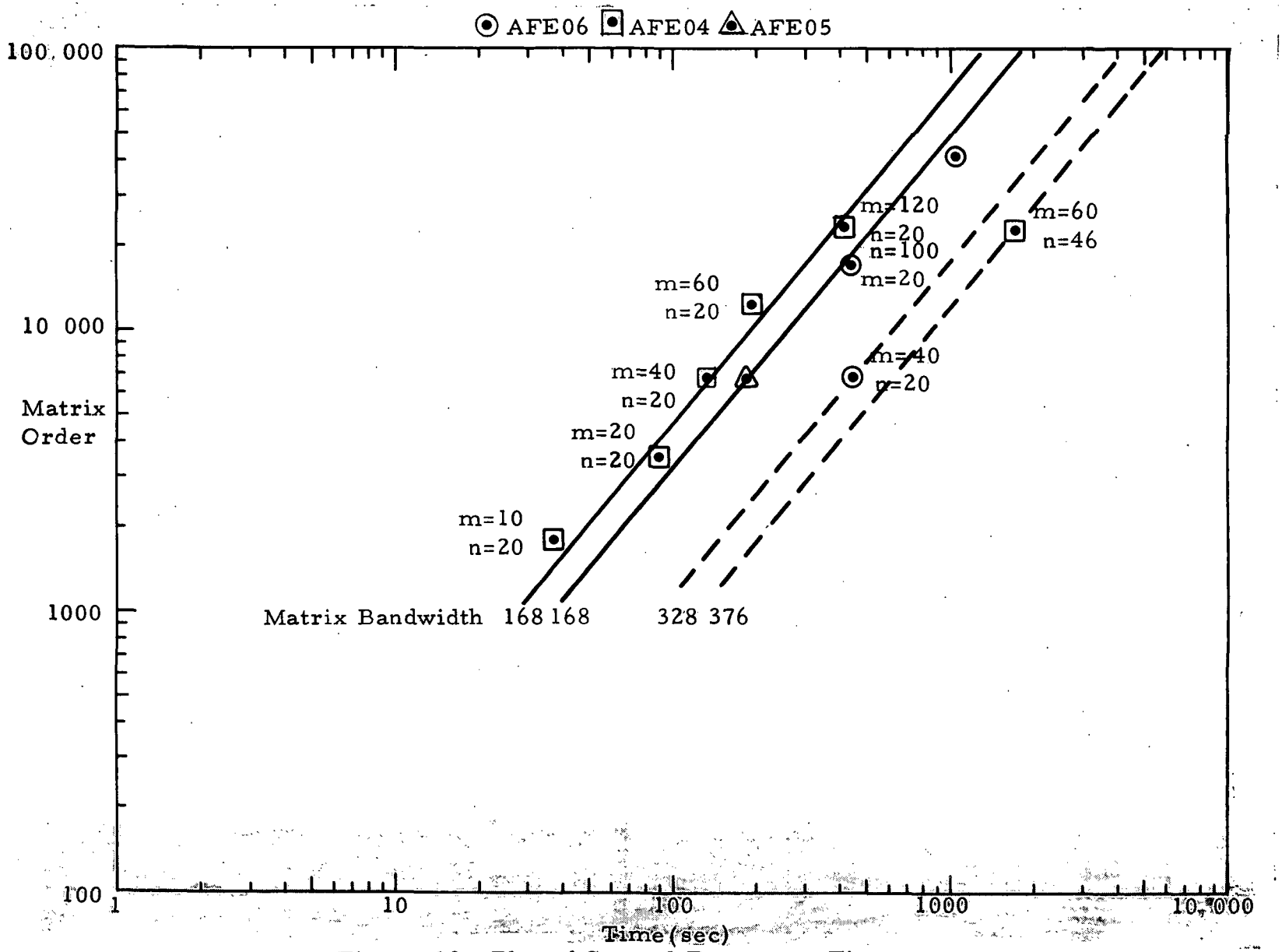

Figure 13. Plot of Central Processor Time (CDC Cyber 175) vs Matrix Order.

4.0 CONCLUSIONS

The objective of this work was to develop a finite element scheme for the acoustics of aero-engine ducts. The principal difficulty of a direct numerical solution is containing the problem within existing computers and attaining a solution in a reasonable amount of computing time. The mathematical formulation, logical flow sequences, matrix manipulation techniques and a solution scheme to attain the stated objective are described in this report.

Testing and verifying the model is complicated by the fact that available alternative analyses possess only a small portion of its total capability. With this restriction in mind, testing of the model was carried out in such a manner in order to compare results with several alternative analyses. Results of the testing program are satisfactory with the model showing good convergence characteristics over a wide range of conditions.

Specific parameters such as spatial acoustic pressure variations and duct attenuation were compared with alternative analyses. General trends such as refraction of acoustic energy by a mean flow shear layer were verified.

An aspect of the model likely to yield interesting information on acoustic design of aero-engine ducts is its ability to be used in conjuction with optimization studies where parameters such as duct shape, size and shape of centerbodies, and multisection or continuous acoustic liners may be varied. Illustrations of the use of the model in this context were presented together with results showing expected and unexpected trends.

Testing of the model in the presence of compressible mean flow has not yet been accomplished. This capability is present in the model but requires linking with a separate analysis to provide mean flow data.

REFERENCES

1. Gladwell, G. M. L., "A Finite Element Method for Acoustics," Paper L33, 5th International Congress on Acoustics, Liege, September 1965.

2. Gladwell, G. M. L., "A Variational Formulation of Damped Acousto-Structural Vibration Problems," Journal of Sound and Vibration, Vol. 4, Number 2, pp. 172-186, 1966.

3. Gladwell, G. M. L., "Variational Finite Element Calculation of the Acoustic Response of a Rectangular Plate," Journal of Sound and Vibration, Volume 14, Number 1, pp. 115-135, 1971.

4. Craggs, A., "Computation of the Response of Coupled Plate-Acoustic Systems Using Plate Finite Elements and Acoustic Volume-Displacement Theory," Journal of Sound and Vibration, Volume 18, Number 2, pp. 235-245, 1971.

5. Craggs, A., "The Use of Simple Three Dimensional Acoustic Finite Elements for Determining the Natural Modes and Frequencies of Complex Shaped Enclosures," Journal of Sound and Vibration, Volume 23, Number 3, pp. 331-339, 1972.

6. Shuku, T., and Ishihara, K., "The Analysis of the Acoustic Field in Irregularly Shaped Rooms by the Finite Element Method," Journal of Sound and Vibration, Volume 29, Number 1, pp. 67-76, 1973.

7. Craggs, A., "An Acoustic Finite Element Approach for Studying Boundary Flexibility and Sound Transmission Between Irregular Enclosures," Journal of Sound and Vibration, Volume 30, Number 3, pp. 343-357, 1973.

8. Hunt, J. T., Knittel, M. R., and Barach, D., "Finite Element Approach to Acoustic Radiation from Elastic Structures," Journal of the Acoustical Society of America, Volume 55, Number 2, February 1974.

9. Craggs, A., "A Finite Element Method for Damped Acoustic Systems: an Application to Evaluate the Performance of Reactive Mufflers," Journal of Sound and Vibration, Volume 48, Number 3, October 1976.

10. Mungur, P., and Plumblee, H. E., "Propagation of Sound in a Soft Walled Annular Duct Containing a Sheared Flow," Basic Aerodynamic Noise Research, NASA SP207, July 1969.

11. Mungur, P., and Gladwell, G. M. L., "Acoustic Wave Propagation in a Sheared Fluid Contained in a Duct," Journal of Sound and Vibration, Vo. 9, pp. 28-48, 1969.

12. Baumeister, K. J., and Bittner, E. C., "Numerical Simulation of Noise Propagation in Jet Engine Ducts," NASA Technical Note, NASA TN D-7339, October 1973.

13. Baumeister, K. J., and Rice, E. J., "A Difference Theory for Noise Propagation in Acoustically Lined Ducts with Mean Flow," Institute of Aeronautics and Astronautics Paper 73-1006, 1973.

14. Zorumski, W. E., "Generalized Radiation Impedances and Reflection Coefficients of Circular and Annular Ducts, "Journal of the Acoustical Society of America," Volume 54, Number 6, December 1973.

15. Zorumski, W. E., "Acoustic Theory of Axisymmetric Multisectioned Ducts," NASA Technical Report, NASA TR R419, May 1974.

16. Nayfeh, A. H., Shaker, B. S., and Kaiser, J. E., "Transmission of Sound through Non-Uniform Circular Ducts with Compressible Mean Flows." To be published.

17. Nayfeh, A. H., and Telionis, D. P., "Acoustic Propagation in Ducts with Varying Cross Sections," Journal of the Acoustical Society of America, Volume 54, Number 6, pp. 1654-1661, 1973.

18. Zienkiewicz, O. C., "The Finite Element Method in Engineering Science," McGraw Hill, 1971.

19. Dahlquist, G., and Bjorck, A., "Numerical Methods," translated by Ned Anderson, Prentice Hall, 1974.

20. Cantrell, R. H., and Hart, R. W., "Interaction Between Sound and Flow in Acoustic Cavities: Mass, Momentum, and Energy Considerations," Journal of the Acoustical Society of America, Volume 36, pp. 697-706.

21. Morfey, C. L., "Acoustic Energy in Non-Uniform Flows," Journal of Sound and Vibration, Volume 14, Number 2, 1971.

22. Eversman, W., "Energy Flow Criteria for Acoustic Propagation in Ducts with Flow," Journal of the Acoustical Society of America, Volume 49, Number 6, 1971.

23. Lester, H. C., and Posey, J. W., "Optimal One Section and Two Section Circular Sound-Absorbing Duct Liners for Plane Ware and Monopole Sources Without Flow", National Aeronautics and Space Administration Technical Note, NASA TN-D 8348, December 1976.

24. Quinn, D. W., "Attenuation of the Sound Associated with a Plane Ware in a Multisectional Duct," American Institute of Aeronautics and Astronautics, AIAA Paper 74-496, March 1975.

Appendix 1

Area Element Coordinate Transformation

Suppose a vector $\vec{R}$ is given in the global (z, r) system as

$$\vec{R} = z\,\hat{\imath} + r\,\hat{\jmath}$$

$$d\vec{R} = \frac{\partial \vec{R}}{\partial z}\,dz + \frac{\partial \vec{R}}{\partial r}\,dr = \hat{\imath}\,dz + \hat{\jmath}\,dr$$

An element of area in the (z, r) system is given by

$$(\hat{\imath}\,dz) \times (\hat{\jmath}\,dr) = dz\,dr$$

Within the (ξ, η) coordinate system $z = z(\xi, \eta)$, $r = r(\xi, \eta)$

$$d\vec{R} = \frac{\partial \vec{R}}{\partial z}\frac{\partial z}{\partial \xi}\,d\xi + \frac{\partial \vec{R}}{\partial z}\frac{\partial z}{\partial \eta}\,d\eta + \frac{\partial \vec{R}}{\partial r}\frac{\partial r}{\partial \xi}\,d\xi + \frac{\partial \vec{R}}{\partial r}\frac{\partial r}{\partial \eta}\,d\eta$$

Component of $d\vec{R}$ in ξ -direction is $\left(\hat{\imath}\,\frac{\partial z}{\partial \xi} + \hat{\jmath}\,\frac{\partial r}{\partial \xi}\right) d\xi$

Component of $d\vec{R}$ in η -direction is $\left(\hat{\imath}\,\frac{\partial z}{\partial \eta} + \hat{\jmath}\,\frac{\partial r}{\partial \eta}\right) d\eta$

An element of area dA in the (ξ, η) system is given by

$$dA = \left(\hat{\imath}\,\frac{\partial z}{\partial \xi} + \hat{\jmath}\,\frac{\partial r}{\partial \xi}\right) d\xi \times \left(\hat{\imath}\,\frac{\partial z}{\partial \eta} + \hat{\jmath}\,\frac{\partial r}{\partial \eta}\right) d\eta$$

$$= \begin{vmatrix} \frac{\partial z}{\partial \xi} & \frac{\partial r}{\partial \xi} \\ \frac{\partial z}{\partial \eta} & \frac{\partial r}{\partial \eta} \end{vmatrix} d\xi\,d\eta = |J|\,d\xi\,d\eta$$

Appendix 2

Definition of terms used in equations (46) through (49)

$$[\alpha] = r_c [A] + b [F]$$

$$[\beta] = \frac{M_c}{a}\left[r_c\left[[C]-[B]\right] + b\left[[H]-[G]\right]\right] + \frac{M'b}{a}\left[r_c\left[[H]-[G]\right] + b\left[[L]-[K]\right]\right]$$

$$[\gamma] = \frac{1}{a}\left[r_c\left[[C]-[B]\right] + b\left[[H]-[G]\right]\right]$$

$$[\delta] = [A]$$

$$[\mu] = \frac{1}{b}\left[r_c\left[[E]-[D]\right] + b\left[[J]-[I]-[A]\right]\right]$$

and

$$A_{ij} = \int_{-1}^{1}\int_{-1}^{1} N_i N_j \, d\xi \, d\eta = \frac{1}{4}\left(1 + \frac{1}{3}\xi_i \xi_j\right)\left(1 + \frac{1}{3}\eta_i \eta_j\right)$$

$$B_{ij} = \int_{-1}^{1}\int_{-1}^{1} \frac{\partial N_i}{\partial \xi} \cdot N_j \, d\xi \, d\eta = \frac{1}{4}\xi_i\left(1 + \eta_i \eta_j\right)$$

$$C_{ij} = \int_{-1}^{1} N_i N_j \Big|_{\xi=-1}^{\xi=+1} d\eta = \frac{1}{4}\left(\xi_i + \xi_j\right)\left(1 + \frac{1}{3}\eta_i \eta_j\right)$$

$$D_{ij} = \int_{-1}^{1}\int_{-1}^{1} \frac{\partial N_i}{\partial \eta} \cdot N_j \, d\xi \, d\eta = \frac{1}{4}\eta_i\left(1 + \frac{1}{3}\xi_i \xi_j\right)$$

$$E_{ij} = \int_{-1}^{1} N_i N_j \Big|_{\eta=-1}^{\eta=1} d\xi = \frac{1}{4}\left(\eta_i + \eta_j\right)\left(1 + \frac{1}{3}\xi_i \xi_j\right)$$

$$F_{ij} = \int_{-1}^{1}\int_{-1}^{1} \eta N_i N_j \, d\xi \, d\eta = \frac{1}{12}\left(1 + \frac{1}{3}\xi_i \xi_j\right)\left(\eta_i + \eta_j\right)$$

$$G_{ij} = \int_{-1}^{1}\int_{-1}^{1} \eta \frac{\partial N_i}{\partial \xi} \cdot N_j \, d\xi \, d\eta = \frac{1}{12}\xi_i\left(\eta_i + \eta_j\right)$$

$$H_{ij} = \int_{-1}^{1} \eta N_i N_j \Big|_{\xi=-1}^{\xi=1} d\eta = \frac{1}{12}\left(\xi_i + \xi_j\right)\left(\eta_i + \eta_j\right)$$

$$I_{ij} = \int_{-1}^{1}\int_{-1}^{1} \eta \frac{\partial N_i}{\partial \eta} \cdot N_j \, d\xi \, d\eta = \frac{1}{12}\left(1 + \frac{1}{3}\xi_i \xi_j\right)\eta_i \eta_j$$

$$J_{ij} = \int_{-1}^{1} \eta N_i N_j \Big|_{\eta=-1}^{\eta=1} d\xi = \frac{1}{4}\left(1 + \frac{1}{3}\xi_i \xi_j\right)\left(1 + \eta_i \eta_j\right)$$

$$K_{ij} = \int_{-1}^{1}\int_{-1}^{1} \eta^2 \frac{\partial N_i}{\partial \xi} \cdot N_j \, d\xi \, d\eta = \frac{1}{4}\left(\frac{1}{3} + \frac{1}{5}\eta_i \eta_j\right)\xi_i$$

$$L_{ij} = \int_{-1}^{1} \eta^2 N_i N_j \Big|_{\xi=-1}^{\xi=1} d\eta = \frac{1}{4}\left(\xi_i + \xi_j\right)\left(\frac{1}{3} + \frac{1}{5}\eta_i \eta_j\right)$$

where for example, R_{ij} is the (i,j)'th component of the 4 x 4 matrix [A] .

Appendix 3

Abscissae and Weight Coefficients of the Gaussian Quadrature Formula

$$\int_{-1}^{1} f(x)\,dx = \sum_{j=1}^{n} H_j f(a_j)$$

±a	H
n = 2	
0·57735 02691	1·00000 00000
n = 3	
0·77459 66692	0·55555 55555
0·00000 00000	0·88888 88888
n = 4	
0·86113 63115	0·34785 48451
0·33998 10435	0·65214 51548
n = 5	
0·90617 98459	0·23692 68850
0·53846 93101	0·47862 87604
0·00000 00000	0·56888 88888
n = 6	
0·93246 95142	0·17132 44923
0·66120 93864	0·36076 15730
0·23861 91860	0·46791 39345
n = 7	
0·94910 79123	0·12948 49661
0·74153 11855	0·27970 53914
0·40584 51513	0·38183 00505
0·00000 00000	0·41795 91836
n = 8	
0·96028 98564	0·10122 85362
0·79666 64774	0·22238 10344
0·52553 24099	0·31370 66458
0·18343 46424	0·36268 37833
n = 9	
0·96816 02395	0·08127 43883
0·83603 11073	0·18064 81606
0·61337 14327	0·26061 06964
0·32425 34234	0·31234 70770
0·00000 00000	0·33023 93550
n = 10	
0·97390 65285	0·06667 13443
0·86506 33666	0·14945 13491
0·67940 95682	0·21908 63625
0·43339 53941	0·26926 67193
0·14887 43389	0·29552 42247

Appendix 4

Listing of Subroutine PINDS

```
      SUBROUTINE PINDS(IG,JG,JP,MM,M1,NPAR)
C                 PINDS=*PACKED INDICES*
C  SUBROUTINE TAKES ROW (IG) AND COLUMN (JG) NUMBERS OF AN ELEMENT
C  IN THE UNPACKED GLOBAL MATRIX AND OUTPUTS A COLUMN NUMBER (JP)
C  FOR THAT ELEMENT IN THE PACKED MATRIX.
C  NOTE THAT THE ROW NUMBER OF THE ELEMENT IS THE SAME IN THE PACKED
C  AND UNPACKED MATRICES
C
C    MM=ORDER OF UNPACKED GLOBAL MATRIX
C    M1=NO. OF NODES IN SERIAL NUMBERING (R), DIRECTION
C    NPAR=NO. OF PARAMETERS AT A NODE
C
C    M=NO. OF VARIABLES PER ROW IN SERIAL NUMBERING (R), DIRECTION
C    BW=BANDWIDTH (NO. OF ELEMENTS IN EACH DIAGONAL)
C    IBLOCK= NO. RELATING TO A GROUP OF ELEMENTS TAKEN VERTICALLY
C      (I-WISE OR ROWISE) IN BLOCK STRUCTURE OF TRI-DIAGONAL MATRIX
C
C    ROF= HORIZONTAL (J-WISE OR COLUMNWISE) OFFSET OF FIRST TERM IN
C         RIGHT DIAGONAL
C    COF= ETC. FOR CENTRE DIAGONAL
C    LOF= ETC. FOR LEFT DIAGONAL
C
C
      INTEGER BW,BW1,ROF,COF
      M=M1*NPAR
      BW=NPAR*3
      BW1=BW+1
      IBLOCK=INT((IG-0.999999)/NPAR)+1
      IF(JG.LT.1.OR.JG.GT.MM)GO TO 50
```

```
      COF=(IBLOCK-2)*NPAR
      LOF=COF-M
      ROF=COF+M
      IF(JG.GT.ROF)10,20
   10 IF(JG.LT.ROF+BW1)11,51
   11 JP=JG-ROF+2*BW
      RETURN
   20 IF(JG.GT.COF)21,30
   21 IF(JG.LT.COF+BW1)22,52
   22 JP=JG-COF+BW
      RETURN
   30 IF(JG.GT.LOF)31,54
   31 IF(JG.LT.LOF+BW1)32,53
   32 JP=JG-LOF
      RETURN
   50 IERR=0
      GO TO 60
   51 IERR=1
      GO TO 60
   52 IERR=2
      GO TO 60
   53 IERR=3
      GO TO 60
   54 IERR=4
   60 WRITE(6,100)IERR,IG,JG,JP,MM,M1,NPAR
  100 FORMAT(18H1ERROR STOP NUMBER,I4,20H IN SUBROUTINE PINDS/
     122HOIG,JG,JP,MM,M1,NPAR =,6I10)
      STOP
      END
```

Appendix 5

Termination Boundary Condition

Assume that in the radiation plane $\bar{u}$ varies slowly over an element and that a plane wave solution holds, i.e.,

$$u = u_0 e^{-ikz} \tag{1}$$

$$p = p_0 e^{-ikz} \tag{2}$$

where $$k = \frac{2\pi}{\lambda} = \frac{\omega}{c + \bar{u}} \tag{3}$$

The axial momentum equation (equation (6) was

$$\bar{\rho} i\omega u + (\bar{\rho} v + \rho \bar{v}) \frac{\partial \bar{u}}{\partial r} + \bar{\rho}\, \bar{v} \frac{\partial \bar{u}}{\partial r}$$

$$+ (\bar{\rho} u + \rho \bar{u}) \frac{\partial \bar{u}}{\partial z} + \bar{\rho}\, \bar{u} \frac{\partial u}{\partial z} + \frac{\partial p}{\partial z} = 0$$

assuming that $\frac{\partial \bar{u}}{\partial r}, \bar{v}, \frac{\partial \bar{u}}{\partial z} = 0$, this reduces to

$$\bar{\rho} i\omega u + \bar{\rho}\, \bar{u} \frac{\partial u}{\partial z} + \frac{\partial p}{\partial z} = 0 \tag{4}$$

Substituting (1) and (2) into (4) gives

$$\bar{\rho} u_0 (\omega - k\bar{u}) - p_0 k = 0$$

using (3) $$\frac{u_0}{p_0} = \frac{k}{\bar{\rho}(\omega - k\bar{u})} = \frac{1}{\bar{\rho}(c + \bar{u} - \bar{u})}$$

$$= \frac{1}{\bar{\rho} c} \tag{5}$$

Equation (5) is an admittance condition, and is the approximate boundary condition applied at the radiation plane.

Appendix 6

Insertion of a Noise Source Boundary Condition

Consider the following system of equations:

$$[A]\{x\} = \{B\} \tag{1}$$

i.e.

$$\begin{aligned}
&a_{11}x_1 + a_{12}x_2 \cdots + a_{1k}x_k \cdots + a_{1n}x_n = b_1 \\
&a_{21}x_1 + a_{22}x_2 \cdots + a_{2k}x_k \cdots + a_{2n}x_n = b_2 \\
&\vdots \\
&a_{k1}x_1 + a_{k2}x_2 \cdots + a_{kk}x_k \cdots + a_{kn}x_n = b_k \\
&\vdots \\
&a_{n1}x_1 + a_{n2}x_2 \cdots + a_{nk}x_k \cdots + a_{nn}x_n = b_n
\end{aligned} \tag{2}$$

Inserting the boundary condition

$$x_k = p \tag{3}$$

gives

$$\begin{aligned}
&a_{11}x_1 + a_{12}x_2 \cdots + 0 \cdot x_k \cdots + a_{1n}x_n = b_1 - a_{1k}p \\
&a_{21}x_1 + a_{22}x_2 \cdots + 0 \cdot x_k \cdots + a_{1n}x_n = b_2 - a_{2k}p \\
&\vdots \\
&0 \cdot x_1 + 0 \cdot x_2 \cdots + 1 \cdot x_k \cdots + 0 \cdot x_n = p \\
&\vdots \\
&a_{1n}x_n + a_{n2}x_2 \cdots + 0 \cdot x_k \cdots + a_{nn}x_n = b_n - a_{nk}p
\end{aligned} \tag{4}$$

Appendix 7

I. Insertion of an Admittance Boundary Condition

Consider the following system of equations:

$$[A]\{X\} = \{B\}$$

i.e.

$$\begin{aligned}
&a_{11}X_1 + a_{12}X_2 \cdots + a_{1k}X_k \cdots + a_{1\ell}X_\ell \cdots + a_{1m}X_m \cdots + a_{1n}X_n = b_1\\
&a_{21}X_1 + a_{22}X_2 \cdots + a_{2k}X_k \cdots + a_{2\ell}X_\ell \cdots + a_{2m}X_m \cdots + a_{2n}X_n = b_2\\
&\vdots\\
&a_{k1}X_1 + a_{k2}X_2 \cdots + a_{kk}X_k \cdots + a_{k\ell}X_\ell \cdots + a_{km}X_m \cdots + a_{kn}X_n = b_k\\
&\vdots\\
&a_{\ell 1}X_1 + a_{\ell 2}X_2 \cdots + a_{\ell k}X_k \cdots + a_{\ell\ell}X_\ell \cdots + a_{\ell m}X_m \cdots + a_{\ell n}X_n = b_\ell\\
&\vdots\\
&a_{m1}X_1 + a_{m2}X_2 \cdots + a_{mk}X_k \cdots + a_{m\ell}X_\ell \cdots + a_{mm}X_m \cdots + a_{mn}X_n = b_m\\
&\vdots\\
&a_{n1}X_1 + a_{n2}X_2 \cdots + a_{nk}X_k \cdots + a_{n\ell}X_\ell \cdots + a_{nm}X_m \cdots + a_{nn}X_n = b_n
\end{aligned} \tag{1}$$

The boundary condition $\beta = \frac{V_n}{p}$, where β is the wall admittance and V_n is the normal component of the acoustic velocity, may be rewritten as

$$V = c_1 p + c_2 u \tag{2}$$

where

$$c_1 = \frac{\beta}{\cos(\theta)}$$

$$c_2 = \tan(\theta) \tag{3}$$

and θ is the angle between the wall and the Z-axis (see Figure 7-1).

Suppose $X_k = u \qquad X_\ell = V \qquad X_m = p$

then

$$X_\ell = c_1 X_m + c_2 X_k \tag{4}$$

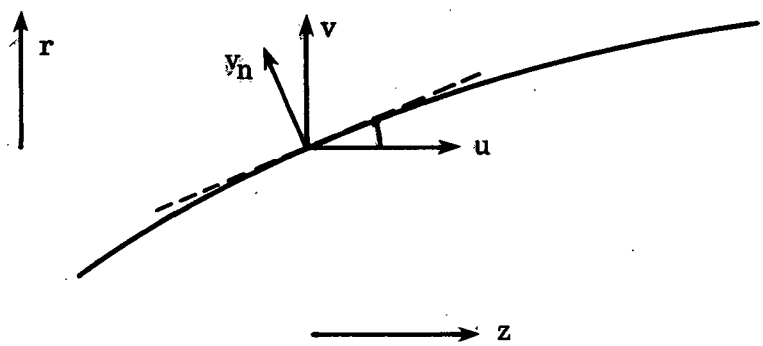

Figure 7-1 Orientation of Acoustic Velocities and Boundary Wall.

Substituting (4) in (1) gives

$$a_{11}x_1 + a_{12}x_2 \cdots + (a_{1k} + c_2 a_{1\ell})x_k \cdots + 0\cdot x_\ell \cdots + (a_{1m} + c_1 a_{1\ell})x_m \cdots + a_{1n}x_n = b_1$$
$$a_{21}x_1 + a_{22}x_2 \cdots + (a_{2k} + c_2 a_{2\ell})x_k \cdots + 0\cdot x_\ell \cdots + (a_{2m} + c_1 a_{2\ell})x_m \cdots + a_{2n}x_n = b_2$$
$$\vdots$$
$$a_{k1}x_1 + a_{k2}x_2 \cdots + (a_{kk} + c_2 a_{k\ell})x_k \cdots + 0\cdot x_\ell \cdots + (a_{km} + c_1 a_{k\ell})x_m \cdots + a_{kn}x_n = b_k$$
$$\vdots$$
$$0\cdot x_1 + 0\cdot x_2 \cdots - c_2 x_k \cdots + x_\ell \cdots - c_1 x_m \cdots + 0\cdot x_n = 0$$
$$\vdots$$
$$a_{m1}x_1 + a_{m2}x_2 \cdots + (a_{mk} + c_2 a_{m\ell})x_k \cdots + 0\cdot x_\ell \cdots + (a_{mm} + c_1 a_{m\ell})x_m \cdots + a_{mn}x_n = b_m$$
$$\vdots$$
$$a_{n1}x_1 + a_{n2}x_2 \cdots + (a_{nk} + c_2 a_{n\ell})x_k \cdots + 0\cdot x_\ell \cdots + (a_{nm} + c_1 a_{n\ell})x_m \cdots + a_{nn}x_n = b_n$$

Clearly, we may have chosen to eliminate either u or b instead of V in the process above. The choice of which parameter to eliminate depends on the numerical values of c_1 and c_2. If in equations (3), for example, θ tended towards $\frac{\pi}{2}$, unreliable results will be obtained from equations (5).

Appendix 8

Linear Numerical Flux Integration

In order to complete acoustic flux it is necessary to evaluate the intensity distribution over a plane. This may be done numerically in the following manner (assuming $(r_2 - r_1)$ is small) :

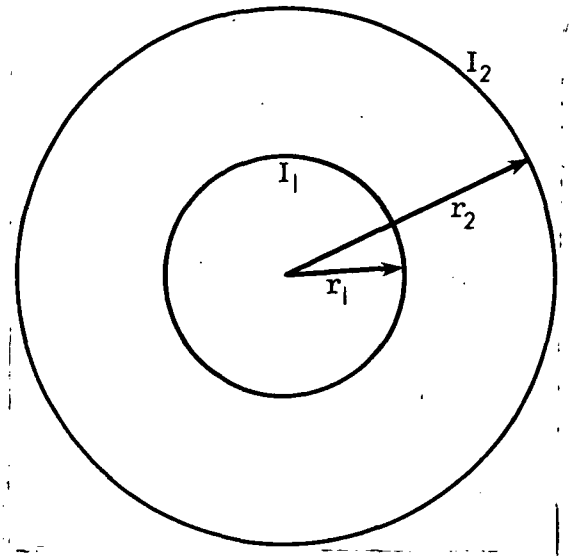

$$a r_1 + b = I_1$$

$$a r_2 + b = I_2$$

$$a(r_2 - r_1) = I_1 - I_2$$

$$a = \frac{I_1 - I_2}{r_1 - r_2}$$

$$b = I_1 - \frac{(I_1 - I_2) r_1}{r_1 - r_2}$$

We want to evaluate

$$F = \int_{r_1}^{r_2} I(r) \cdot 2\pi r \, dr$$

$$= \int_{r_1}^{r_2} (ar + b) \cdot 2\pi r \, dr$$

$$= 2\pi \left(\frac{a r^3}{3} + \frac{b r^2}{2} \right)_{r_1}^{r_2}$$